

Evaluation of CO₂-EOR Performance and Storage Mechanisms: FWU Case Study

W. Ampomah, Qian Sun*, E.J. Kutsienyo and R. Balch

PRESENTATION OUTLINE

- Project Overview
- Reservoir Simulation & History Matching
- Storage Mechanisms Evaluation
 - Structural Trapping
 - Solubility Trapping
 - Geochemical Trapping
- Conclusive Remarks

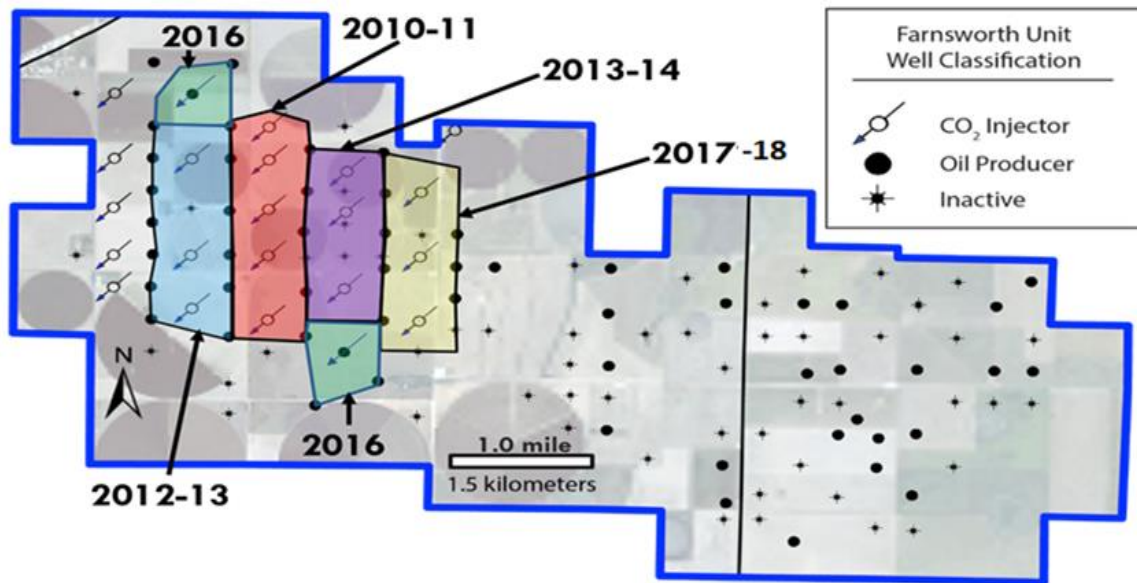
SOUTHWEST REGIONAL CARBON SEQUESTRATION PARTNERSHIP FWU – LARGE-SCALE EOR- CCUS PROJECT

CO₂ storage volume - February 2019

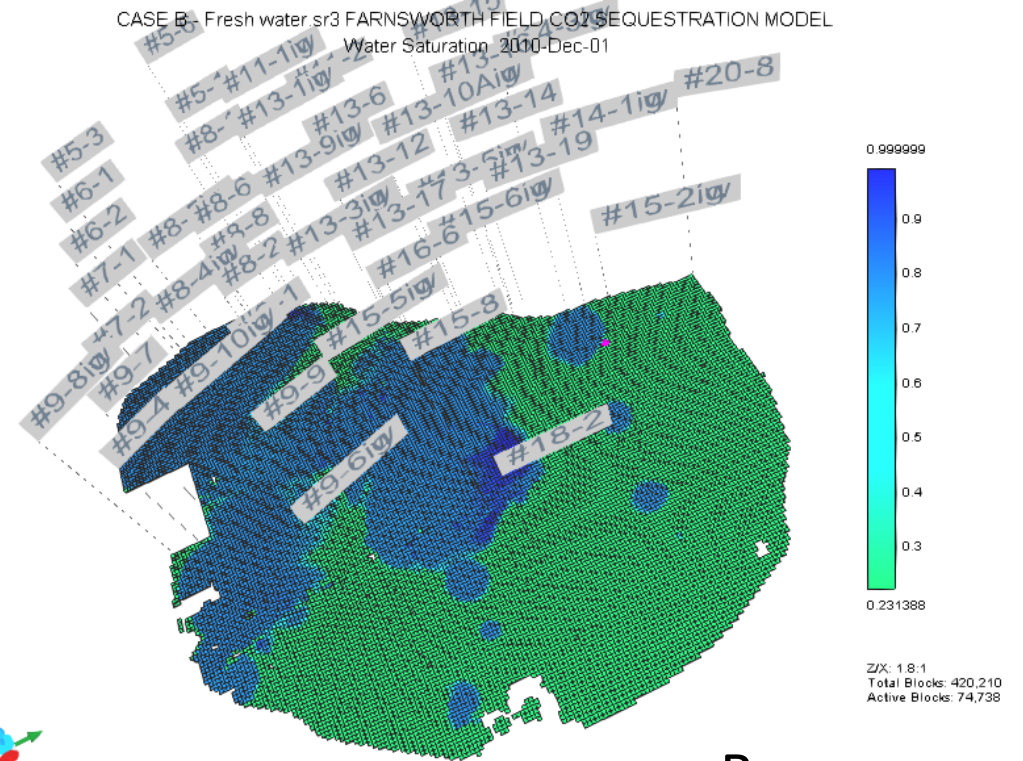
- 1,360,000 metric tons of CO₂ purchased
- 1,260,000 of purchased CO₂ stored within Morrow B sand
- ~ 93% of purchased CO₂ stored
 - Structural-stratigraphic Trapping
 - Residual Trapping
 - Solubility Trapping
 - Mineral Trapping



WEST-HALF INJECTIONS AND PRODUCTION PATTERN OF THE FWU FIELD THAT DESCRIBES THE HISTORY MATCHED PERIOD



A



B

Storage Modelling Workflow

- **Baseline Model (Adopted¹)**

- Primary (1956 – 1964)
- Secondary (1964 – 2010)

- **Parametrizations through Sensitivity Studies:**

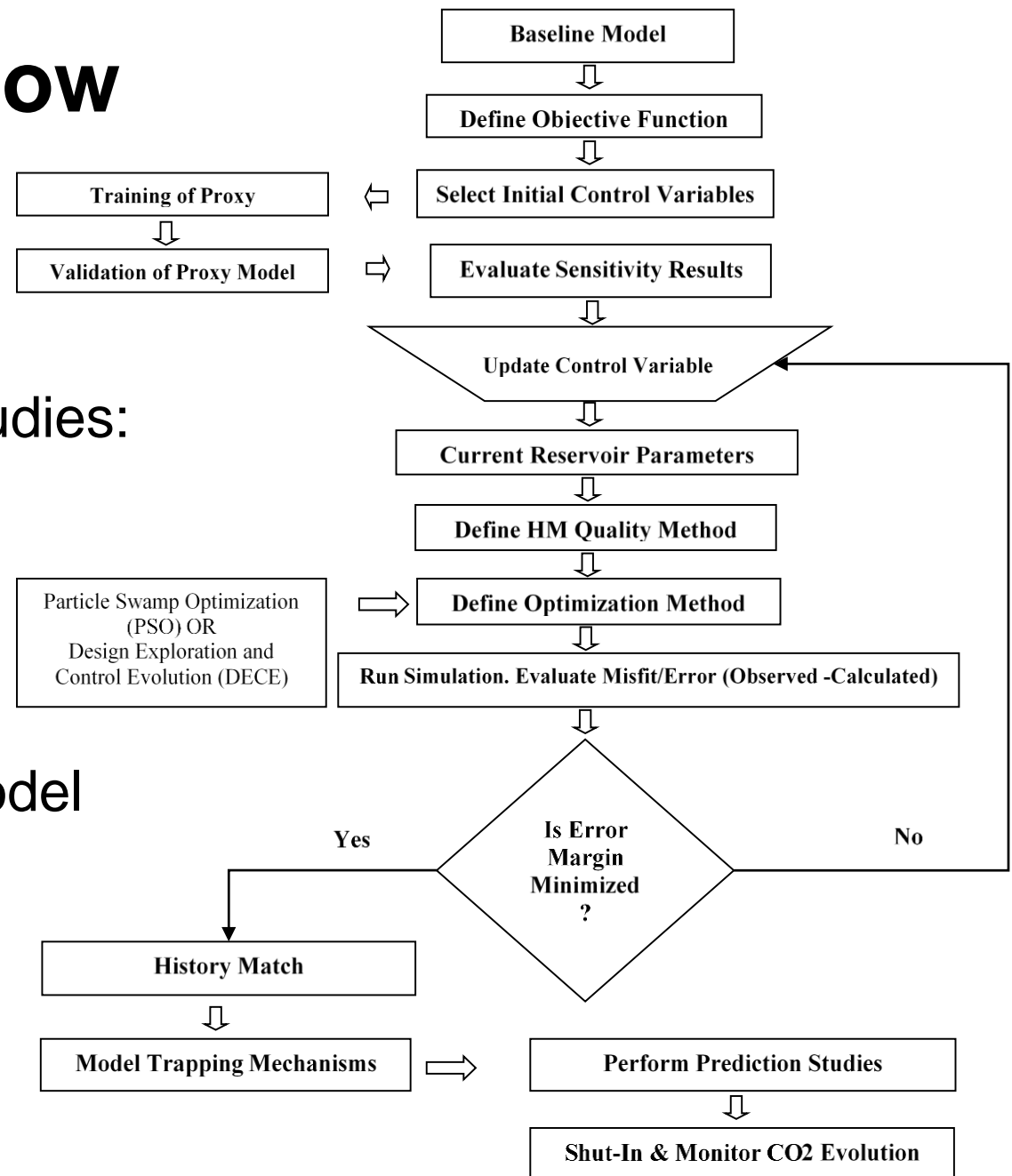
- Spatial permeability distributions
- Relative permeability data

- **History Match (HM) Tertiary Flood**

- CO₂-WAG (2010-2017)

- **Implementations of History-matched Model**

- Development strategies evaluations
- Storage mechanisms evaluations
- CO₂ long-term fate monitoring



PARAMETERIZATION THROUGH SENSITIVITY STUDIES

18 parameters were investigated

175 initial run training and
verification points

236 total simulation experiment
resulted in an acceptable R-
Squared value

Assisted History Matching Observations

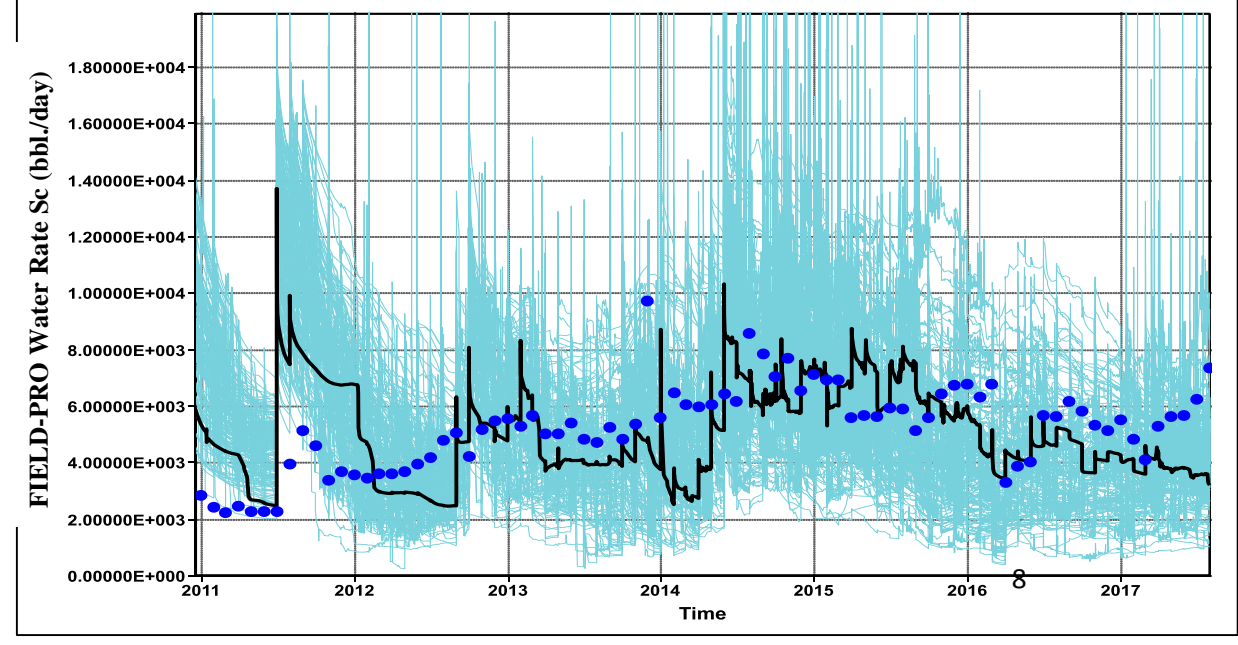
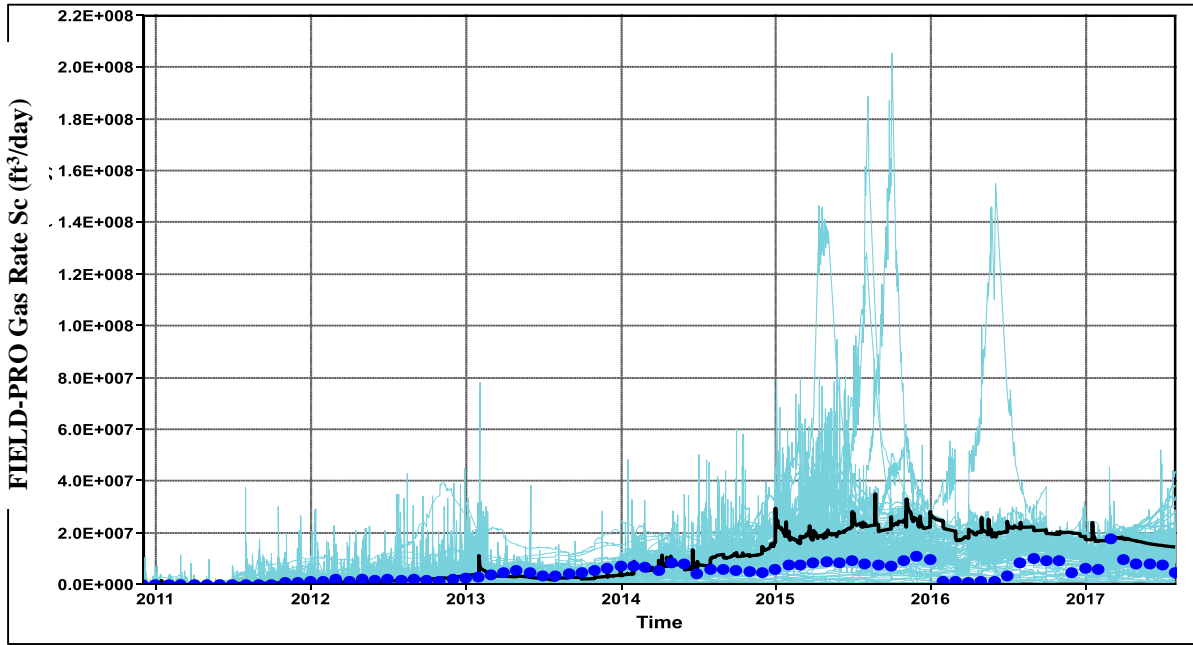
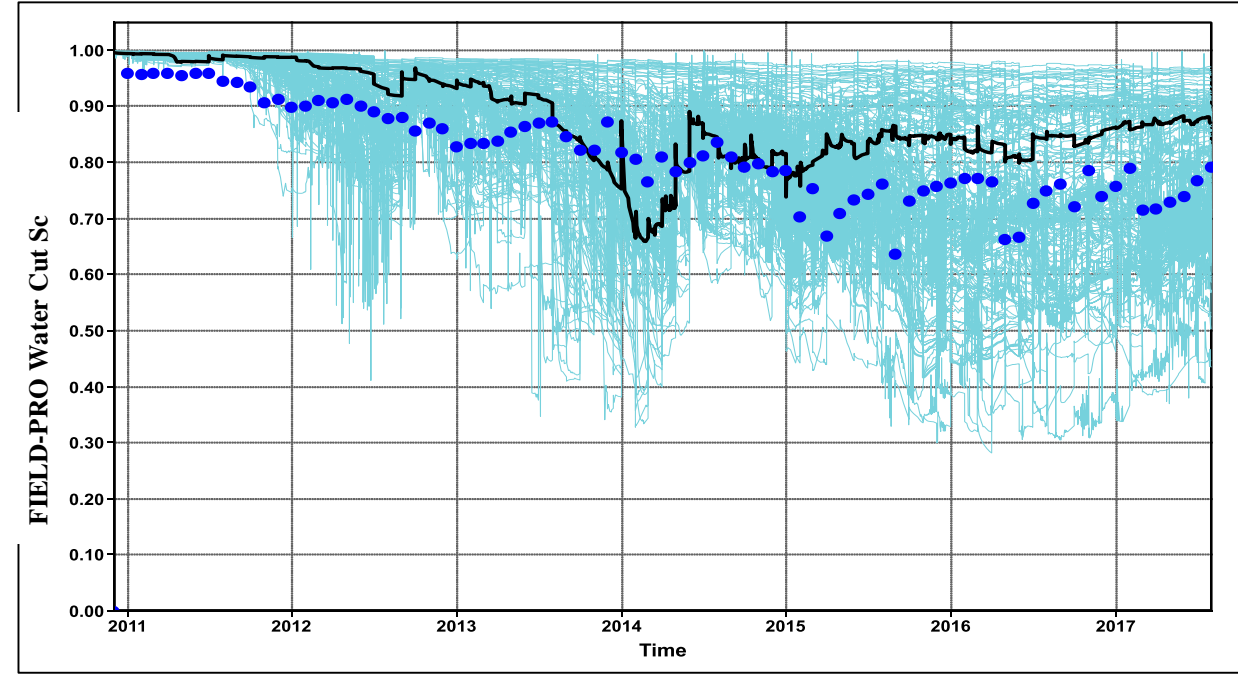
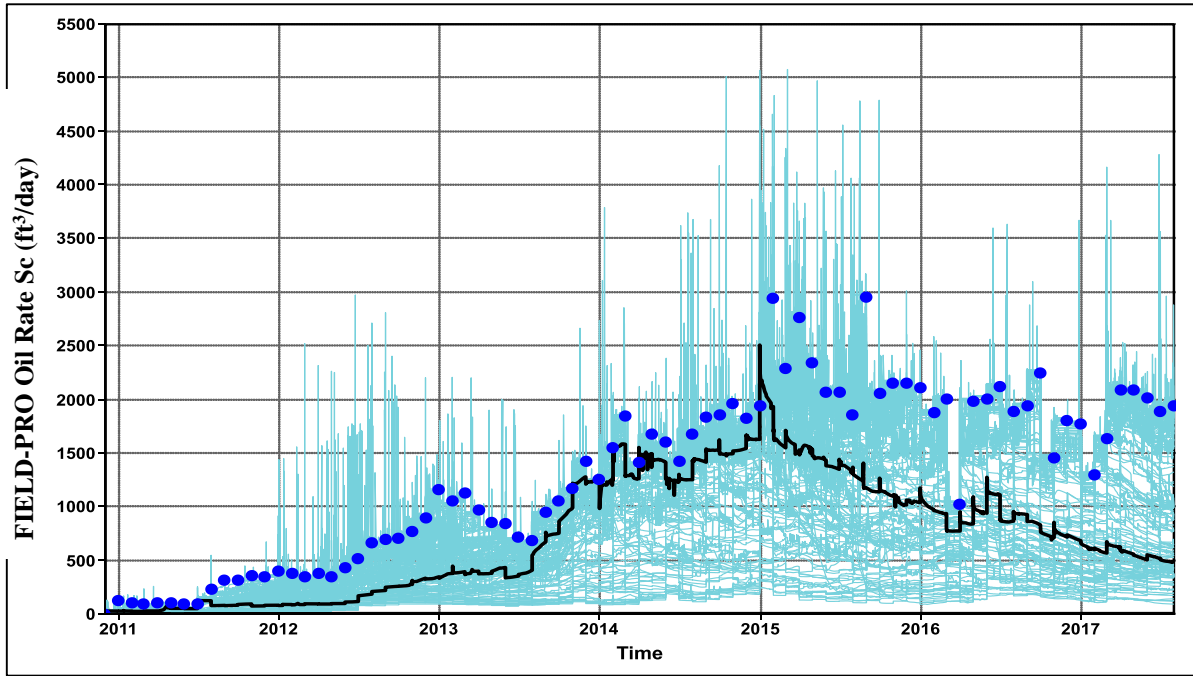
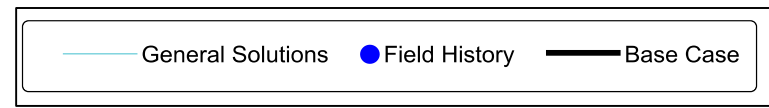
Parameterization with Sensitivity Studies

- All Corey Correlations Parameters
- Permeability (I, J)
- Critical Saturation (e.g. Swcrit)
- Relative perm curve endpoints
 - ✓ Kr at Connate Water(krocw)
 - ✓ Kr at Irreducible oil(krwiro)

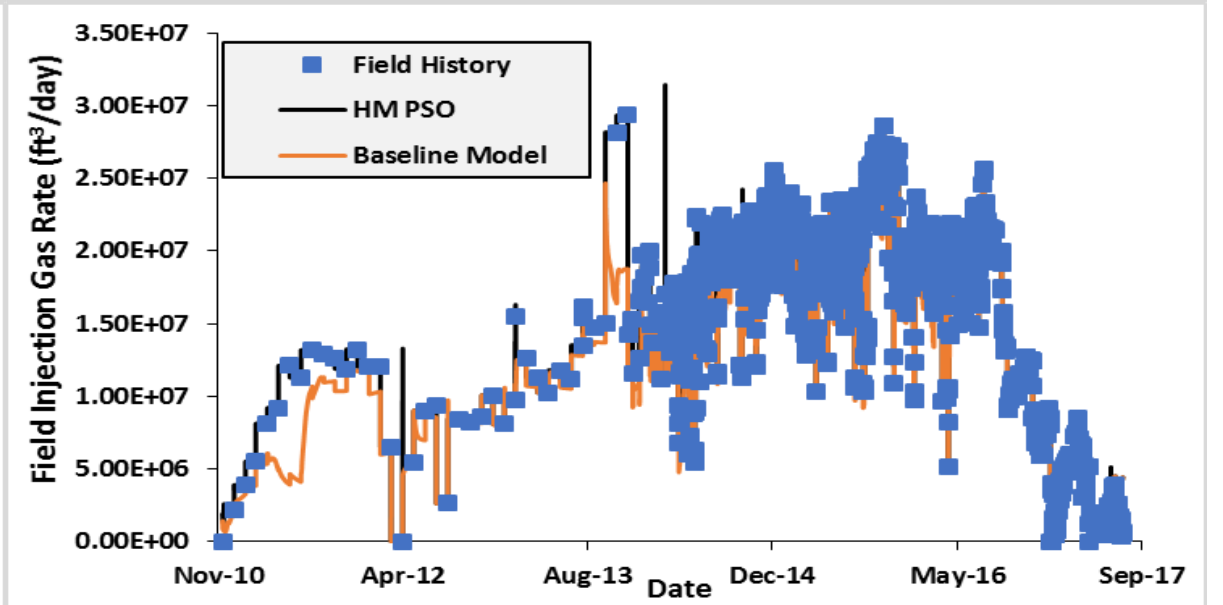
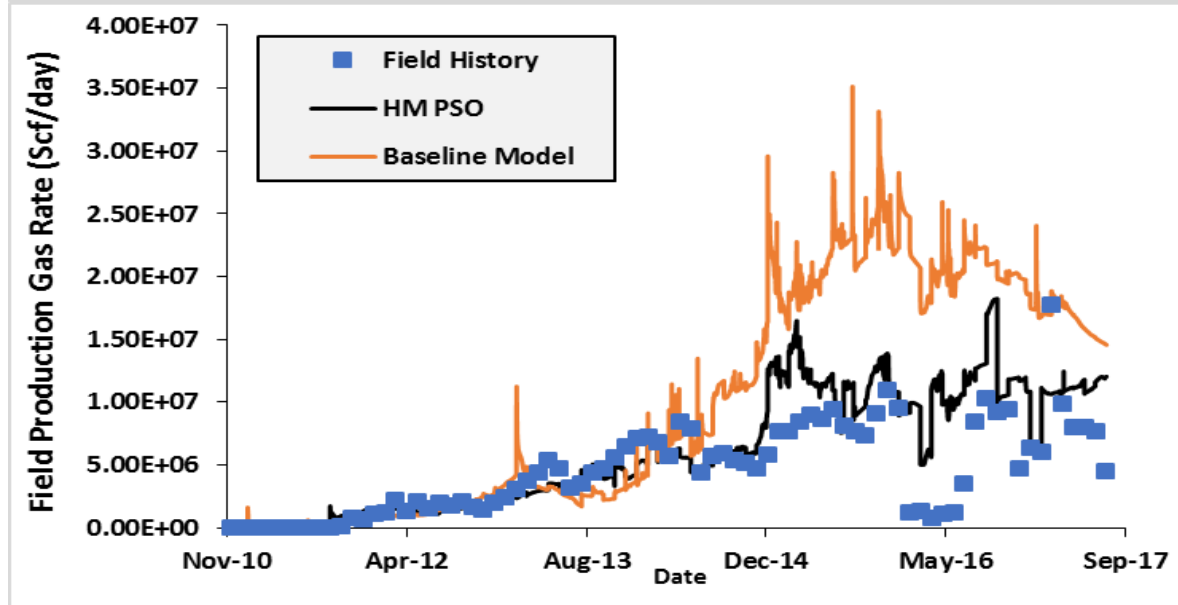
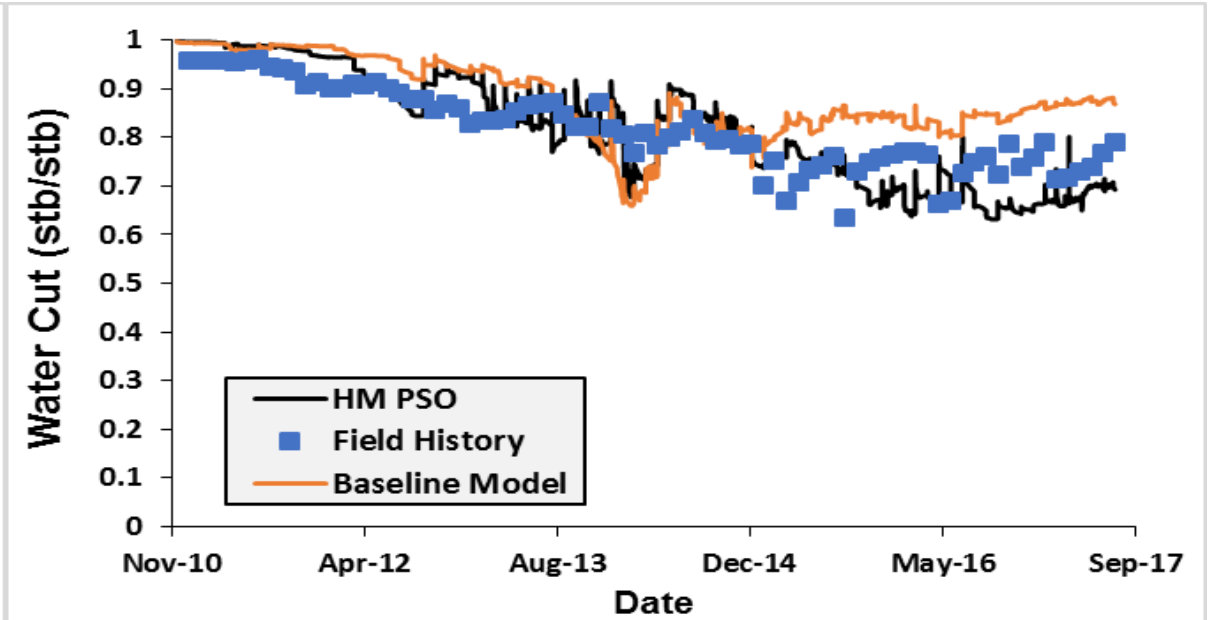
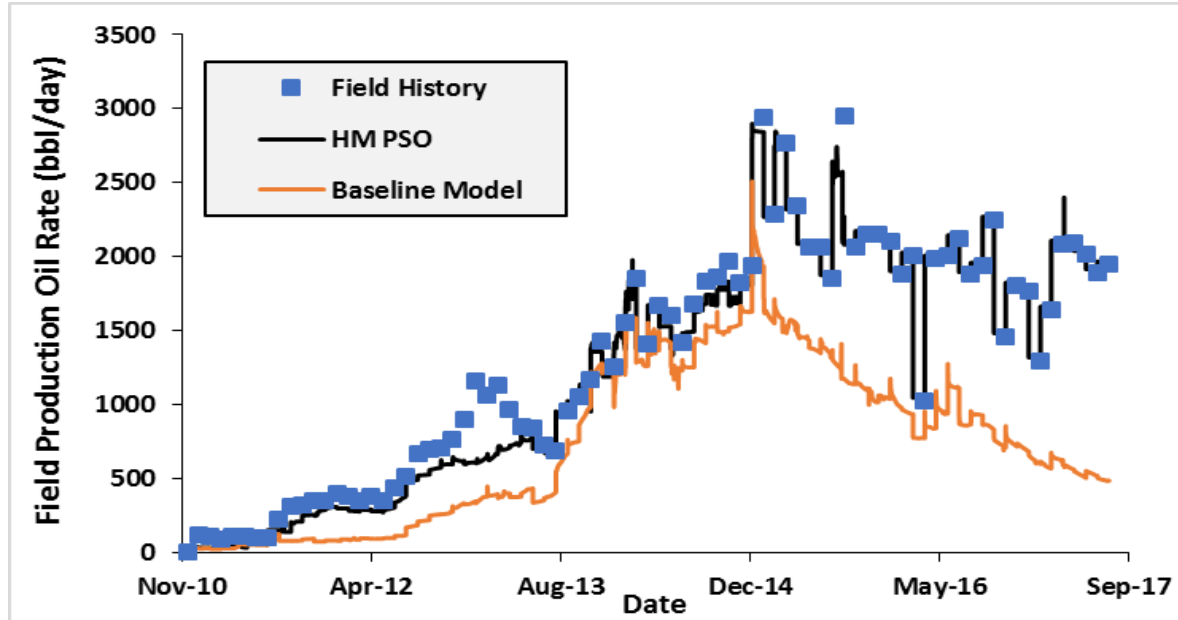
Optimized History Matching Results

- 9.58% in Global History Match Error
 - ✓ 4.5% in cumulative Oil Production Error
 - ✓ 10% cumulative Gas Produce Error
 - ✓ ~6.7% in Average Cumulative Injection Error

Time series plot for all experiments



History Matching Results

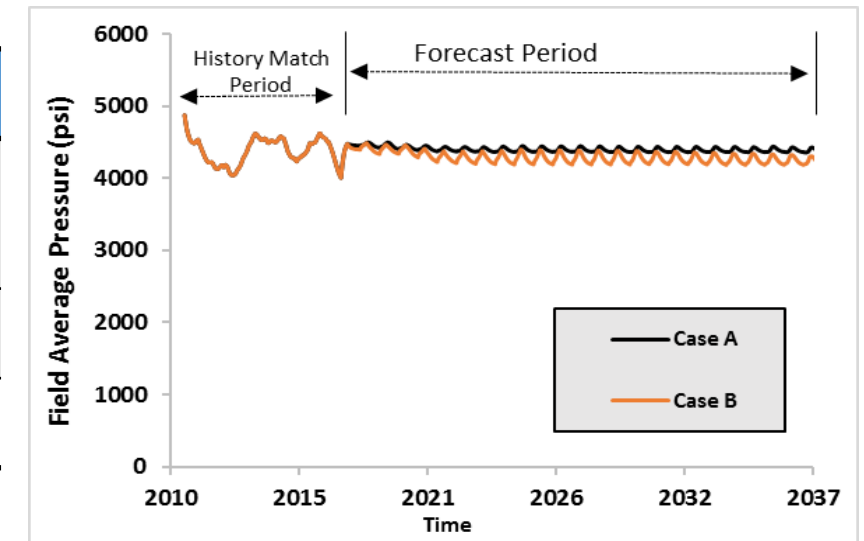
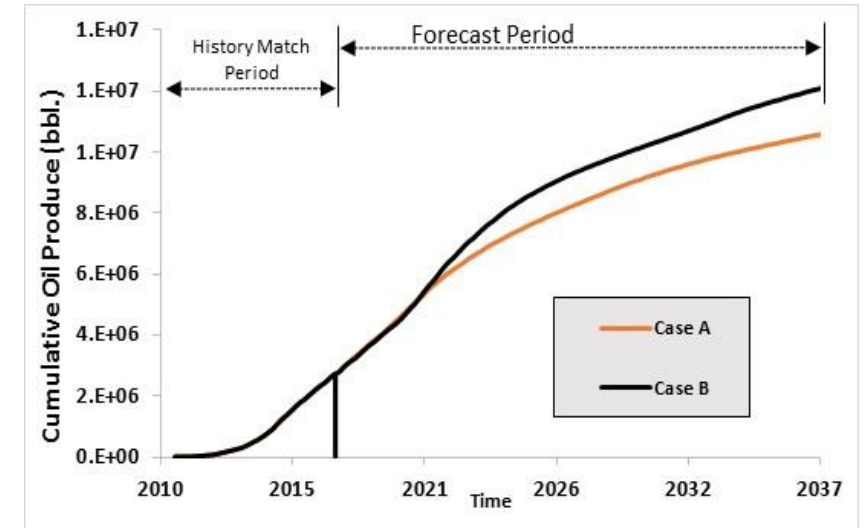


Forecasting Models

- **Case A:** Current WAG patterns (15 wells) and adjacent water injectors (5 wells) with constant daily group target of 20 MMscf/d CO₂ purchase
- **Case B:** Convert all injectors to WAG wells (20 wells) with CO₂ purchase at constant daily group target of 20 MMscf/d CO₂ purchase
- The water-gas injection period ratio is 1:2.

	Oil Recovery (MM bbl.)	Total CO ₂ Injected	Amount of substances of CO ₂ (10 ⁹ g-moles)				
			Structural (Free gas)	Residual Trapped Gas	Solubility Trapped Gas		Total Storage
					Oil	Water	
Case A	10.61	155.4	4.78	4.01	21.85	4.46	35.09
Case B	12.14	155.4	4.67	3.95	28.46	5.88	42.96

Prediction cases (Aug. 2017 – July 2037)



Storage Mechanisms Modeling

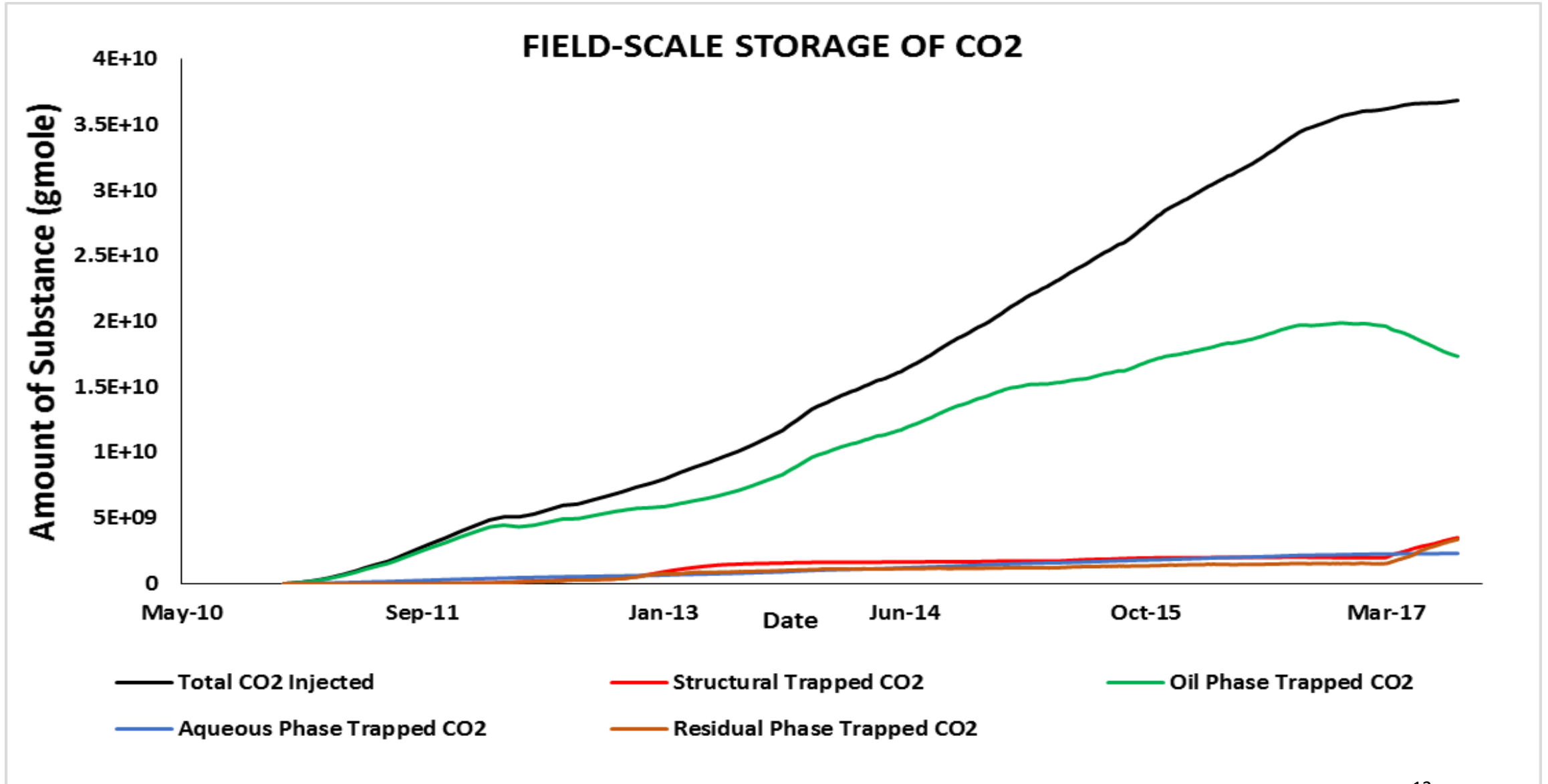
1. GAS SOLUBILITY TRAPPING MODELING

- In this work CO₂ is considered to be soluble in aqueous and oleic phases.
- CO₂-Brine mixture modelled using Henry's Law
- CO₂-Oil Mixture modelled using the Peng-Robison EOS

2. RESIDUAL AND STRUTURAL GAS TRAPPING MODELING

- CO₂ in free phase (supercritical/gaseous phases) is trapped by geological structure of the reservoir.
- Three phase relative permeability hysteresis model is employed to model the residual trapping.

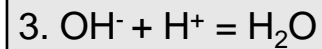
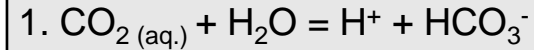
Phase Storage of CO₂ in the Farnsworth Unit – Field



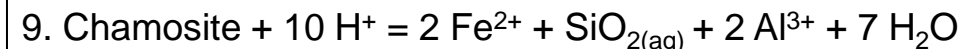
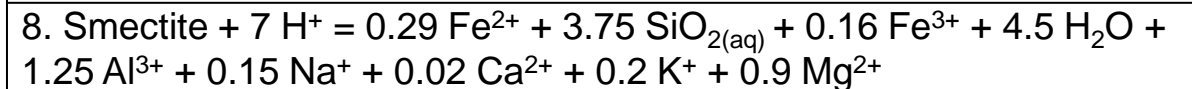
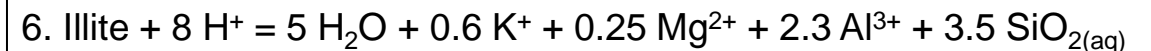
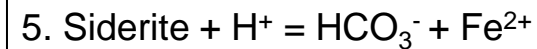
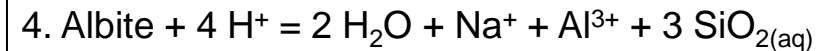
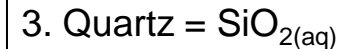
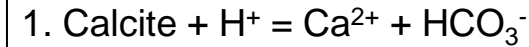
Geochemical Trapping

- Reactive surface areas of the minerals Pan et al., (2016).
- Initial volume fractions and the aqueous species concentrations are taken from Ahmmed et al., (2016).
- The kinetic/activations energy and rate constant taken from Palandri and Kharaka, (2004)
 - At 25°C, using the pH medium of the minerals as described in Pan et al., (2016)
- Mineral volume fractions defined in terms of corresponding bulk volume fraction using the pore volume weighted average porosity (0.142) from the field.

Intra-aqueous chemical equilibrium reactions

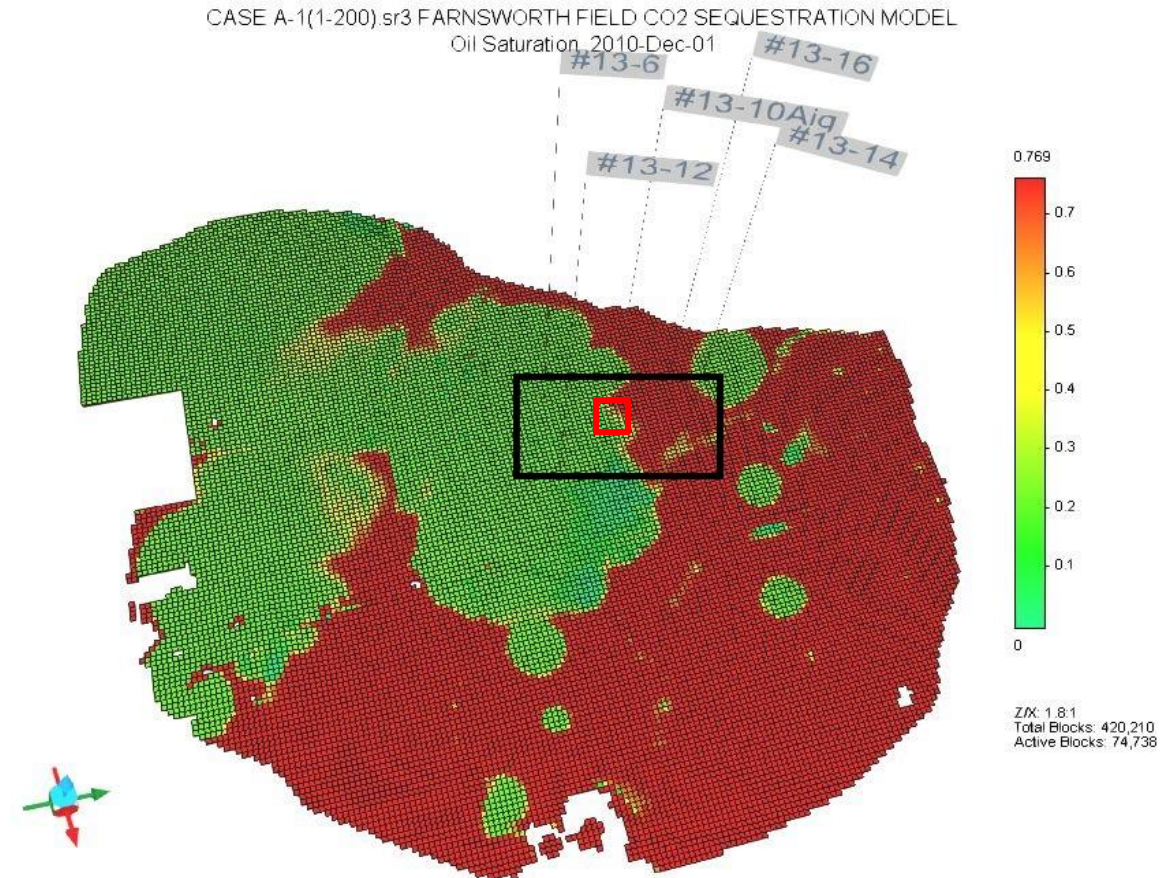


Mineral dissolution/precipitation reactions



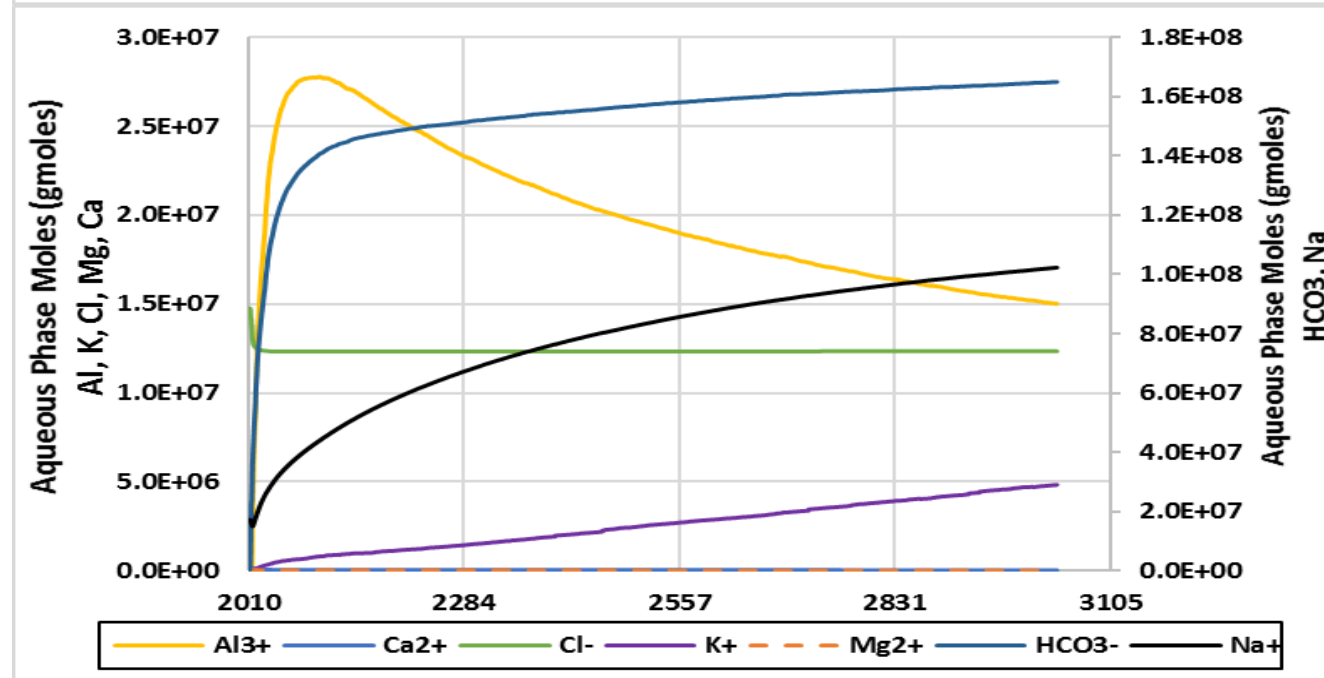
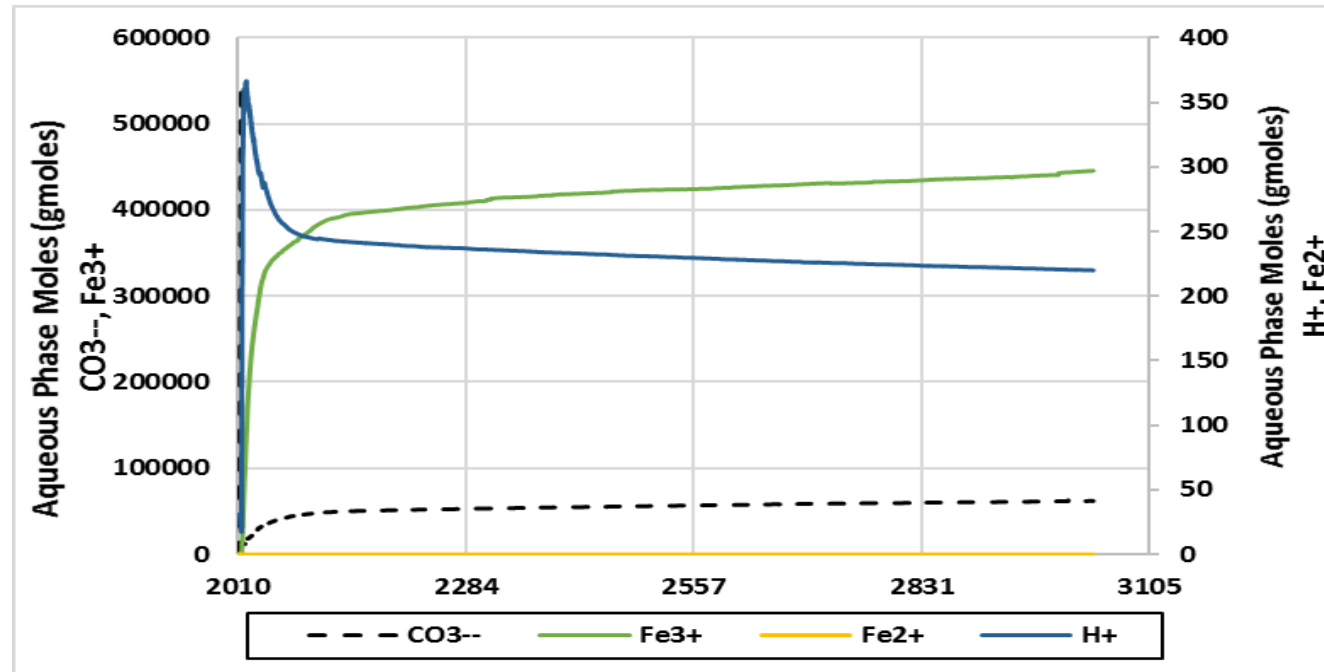
PILOT CASE - Prediction Summary on selected 13-10A pattern

- Mineralization study was performed as a pilot study to relate the chemo-mechanical laboratory experiments prior to field-scale evaluation.
 - Study concentrated around the 13-10A where most cores were collected.
- Mineralization occurs in two forms:
 - Intra-aqueous reactions
 - Dissolution/precipitation reactions
- The simulation model runs for 1,000 years to monitor the fate of the injected CO₂.



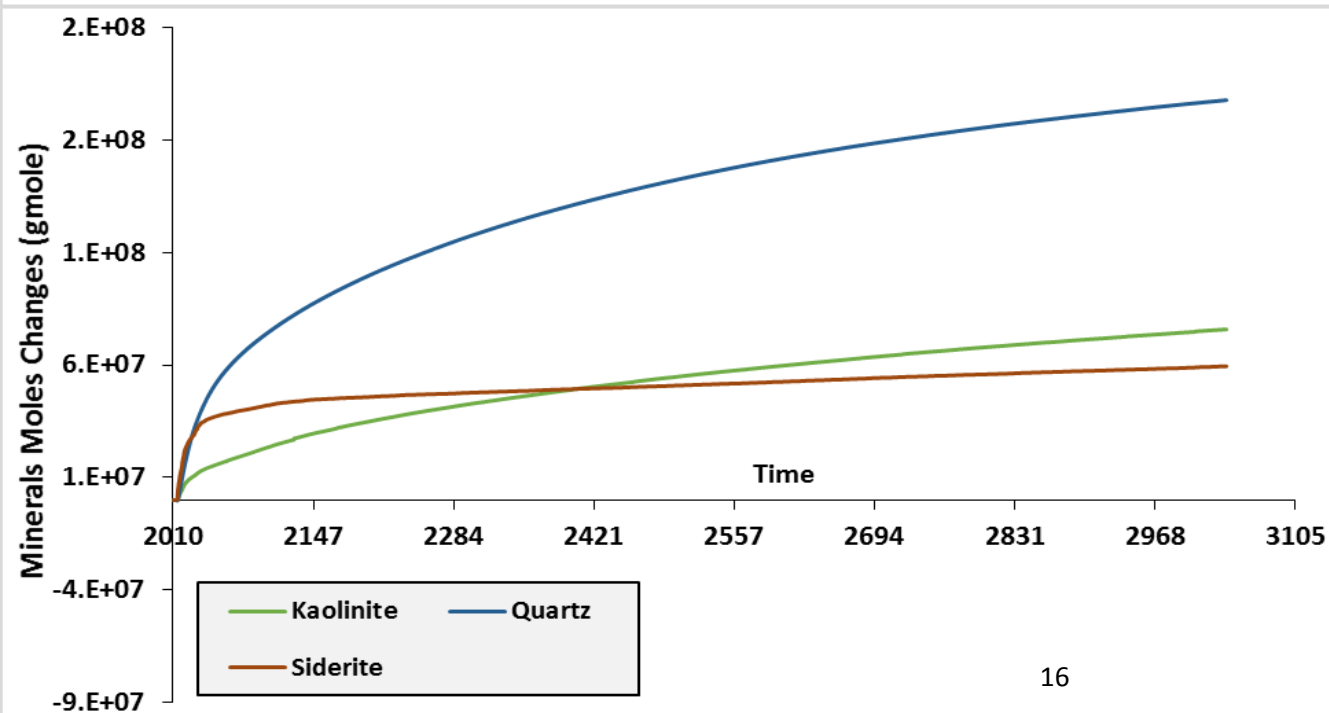
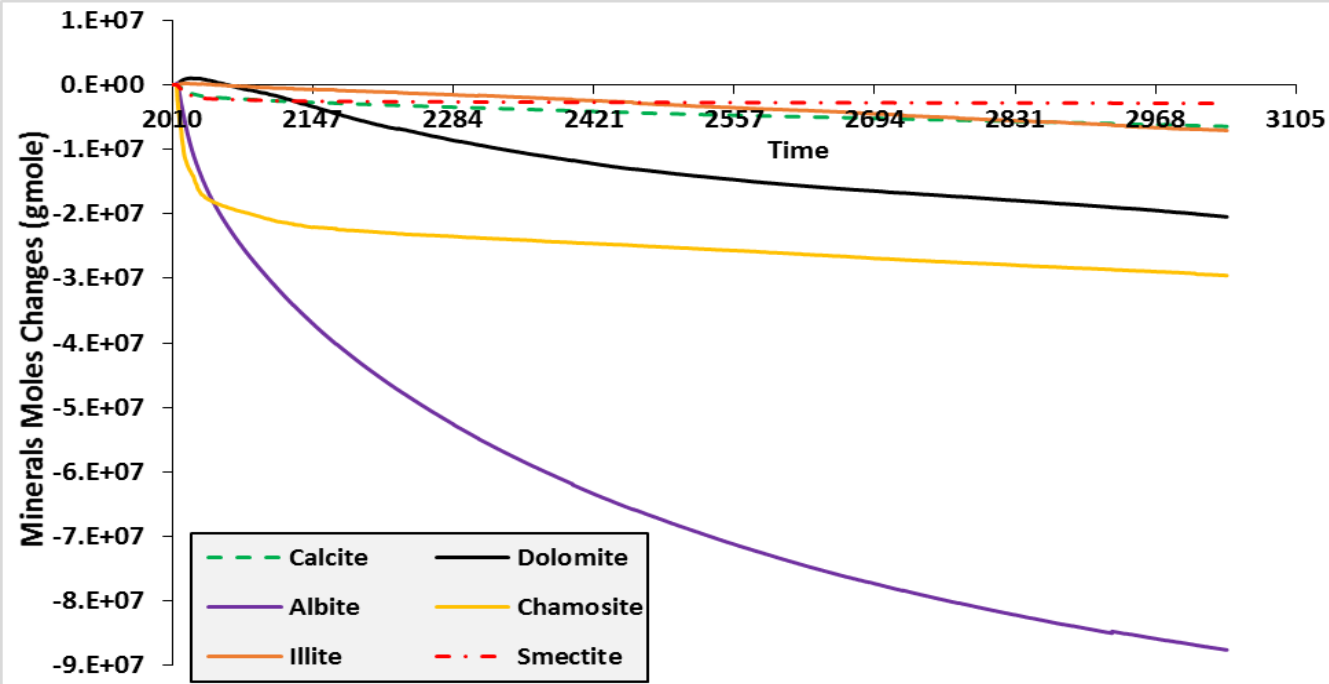
Aqueous Species Evolution

- Evolution of Aqueous Species:
 - Al^{3+} initially increased but later decreased
 - K^+ , CO_3^{2-} , Fe^{3+} , Na^+ , HCO_3^- increased gradually
 - Ca^{2+} , Mg^{2+} , Cl^- , Fe^{2+} continuously decreased
- pH of the in-situ brine initially decreased and later increased relatively

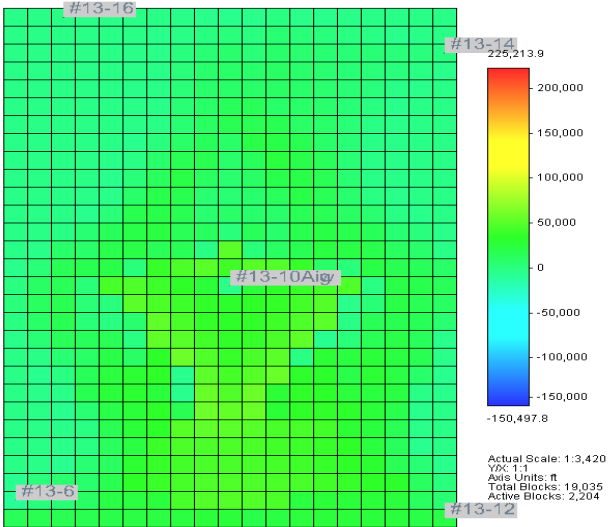


Mineral Evolution in 13-10A area

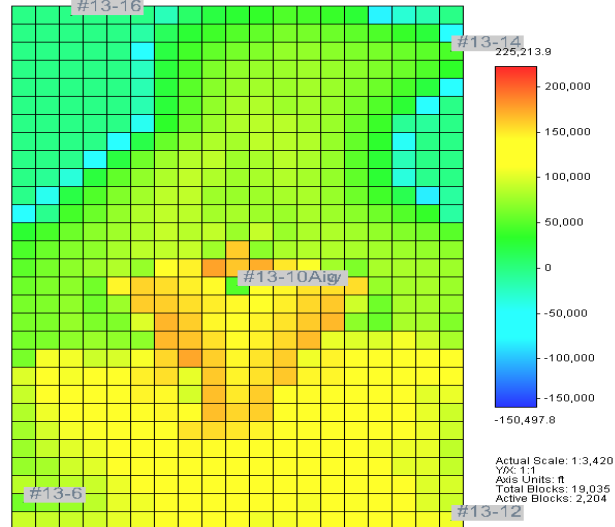
- Dissolution observed in Ankerite-Calcite cements correspond to the chemo-mechanical experiments observed (Ampomah et al. 2016).
- Other Mineral Matrix dissolution and precipitation corresponds with previous studies (for example, Khan et al. 2017).
- Net precipitations is predicted in the reservoir which **correspond to change in porosity.**



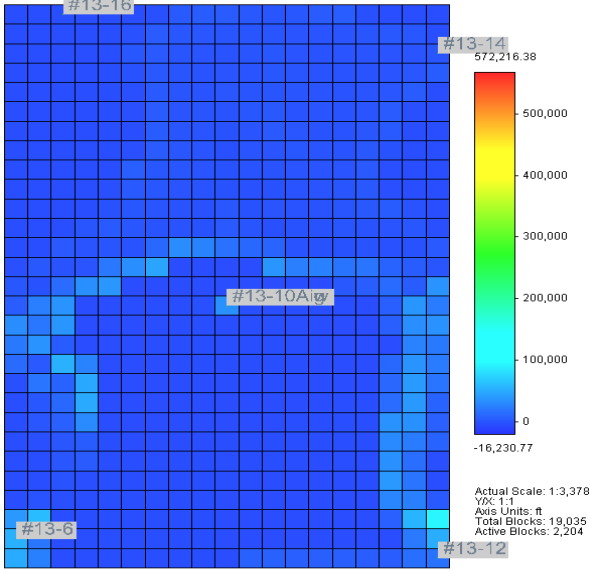
Precipitation Heat maps



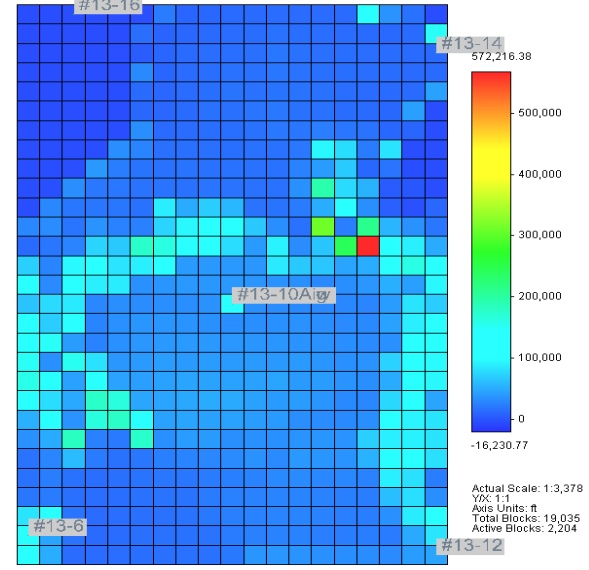
20 years' impact in layer 7 (2037-Dec-01)



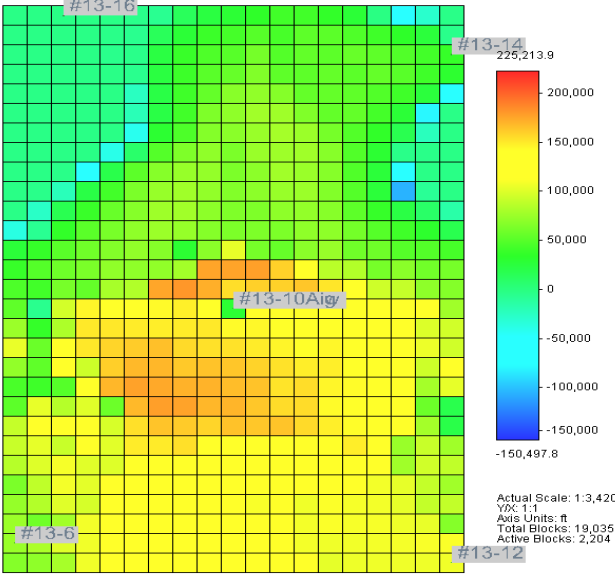
1000 years' impact in layer 7 (3037-Dec-01)



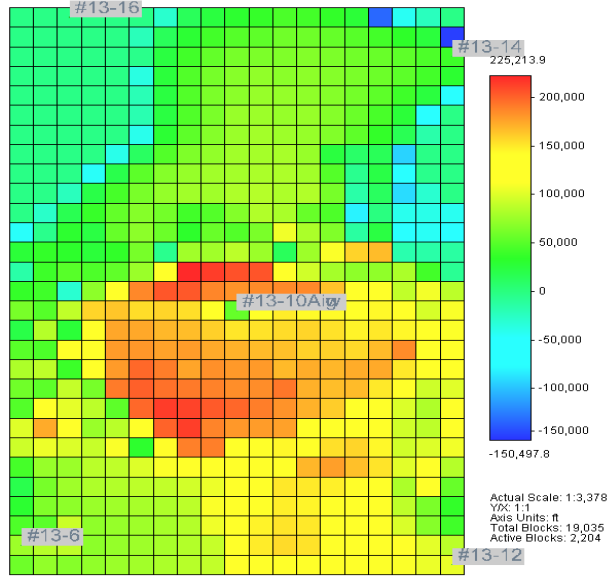
20 years Impact in layers 10 (2037-Dec-01)



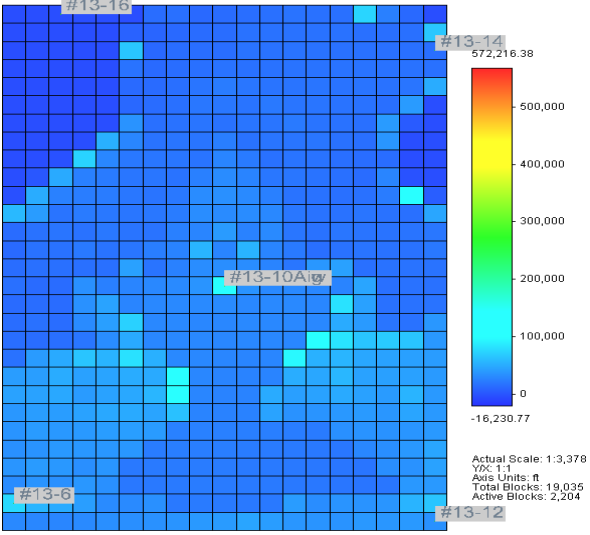
1000 years' impact in layer 7 (3037-Dec-01)



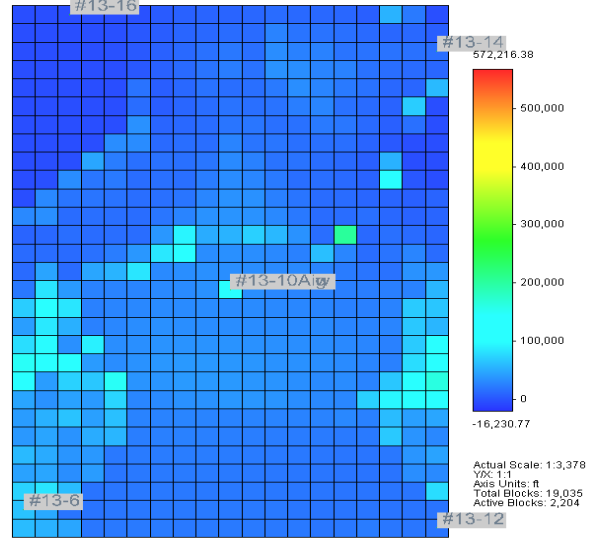
1000 years' impact in layer 9 (3037-Dec-01)



1000 years' impact in layer10 (3037-Dec-01)



1000 years' impact in layer10 (3037-Dec-01)

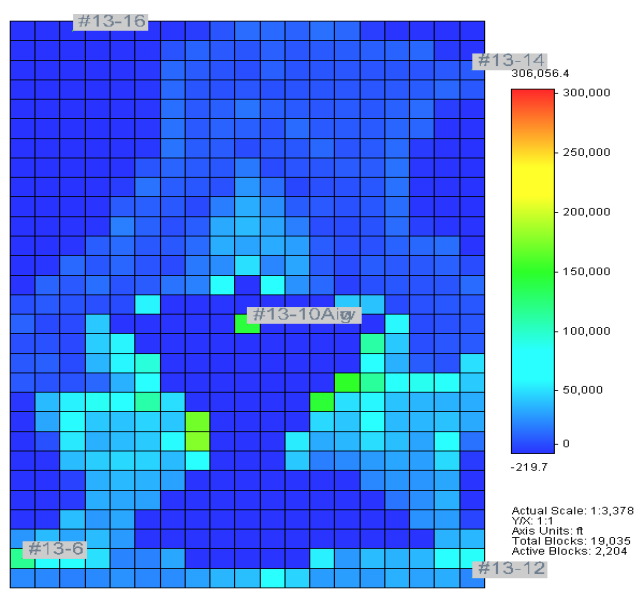


1000 years' impact in layer 9 (3037-Dec-01)

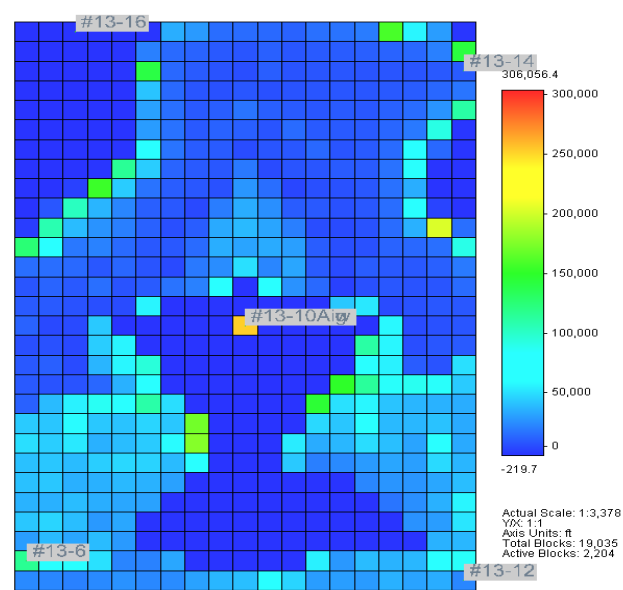
A: Quartz Precipitation

B: Kaolinite precipitations

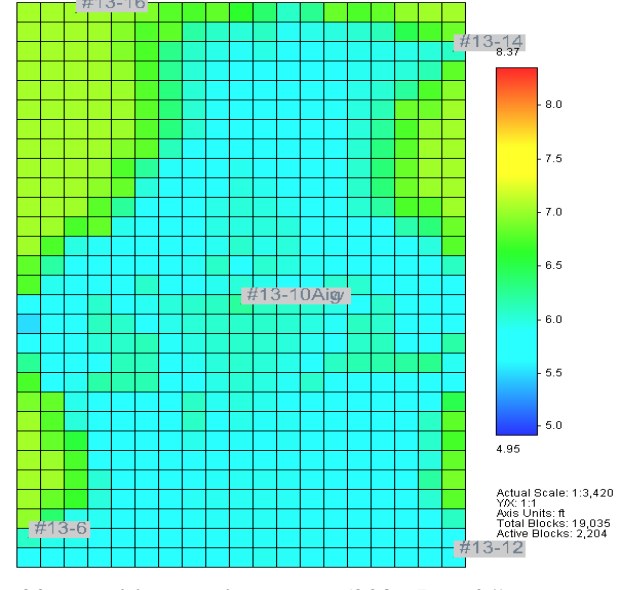
Precipitation and pH value Heat maps



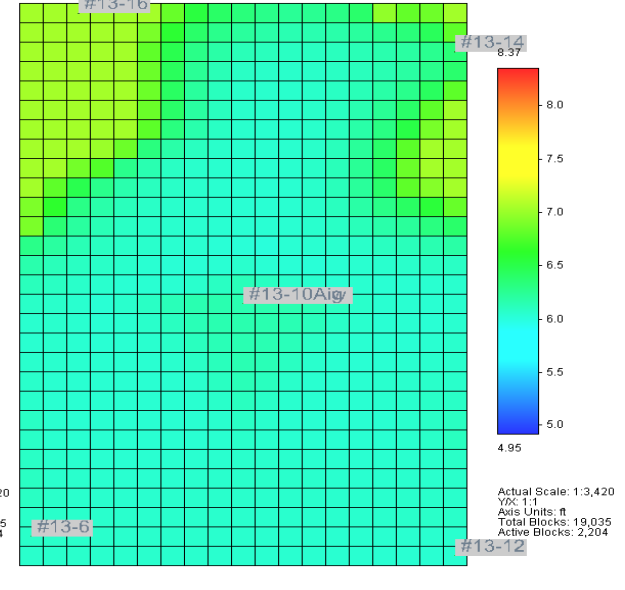
20 years Impact in layers 7 (2037-Dec-01)



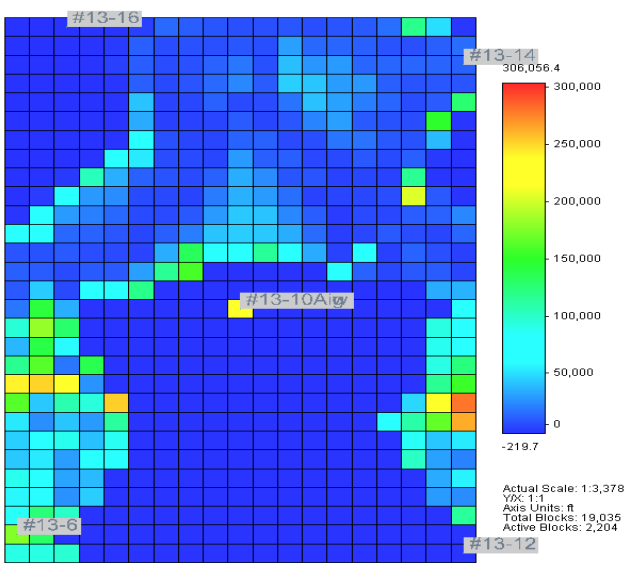
1000 years' impact in layer7 (3037-Dec-01)



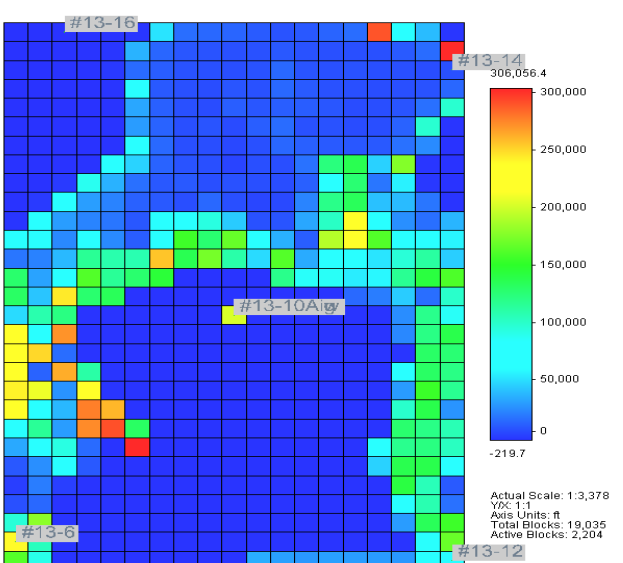
20 years' impact in layer 7 (2037-Dec-01)



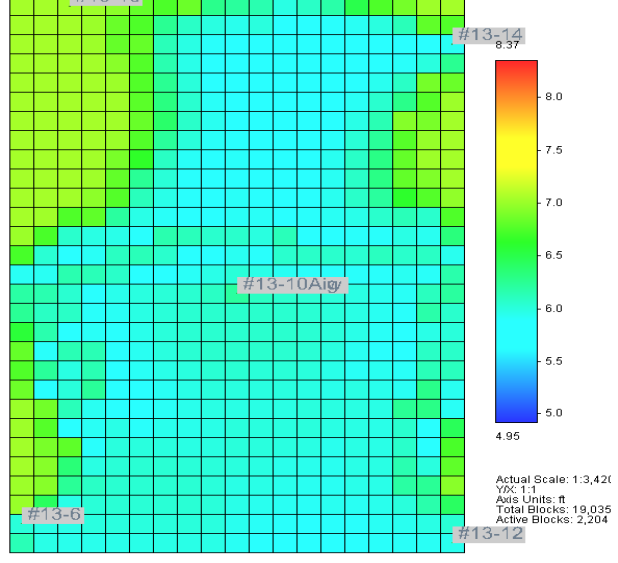
1000 years' impact in layer 7 (3037-Dec-01)



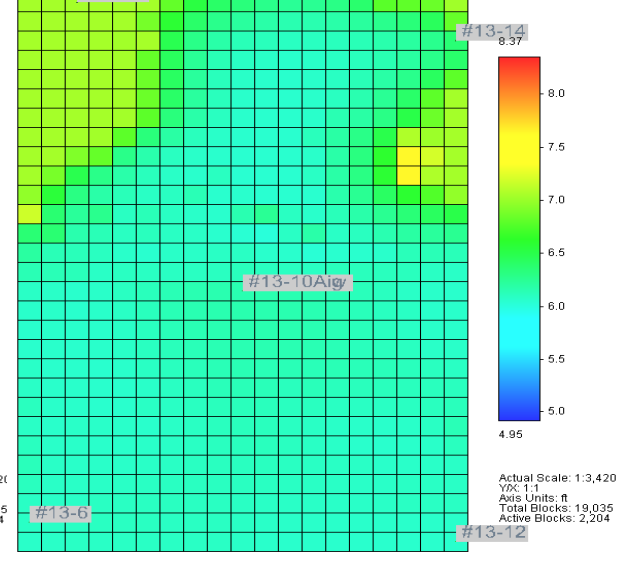
1000 years' impact in layer9 (3037-Dec-01)



1000 years' impact in layer10 (3037-Dec-01)



20 years' impact in layer 10 (2037-Dec-01)

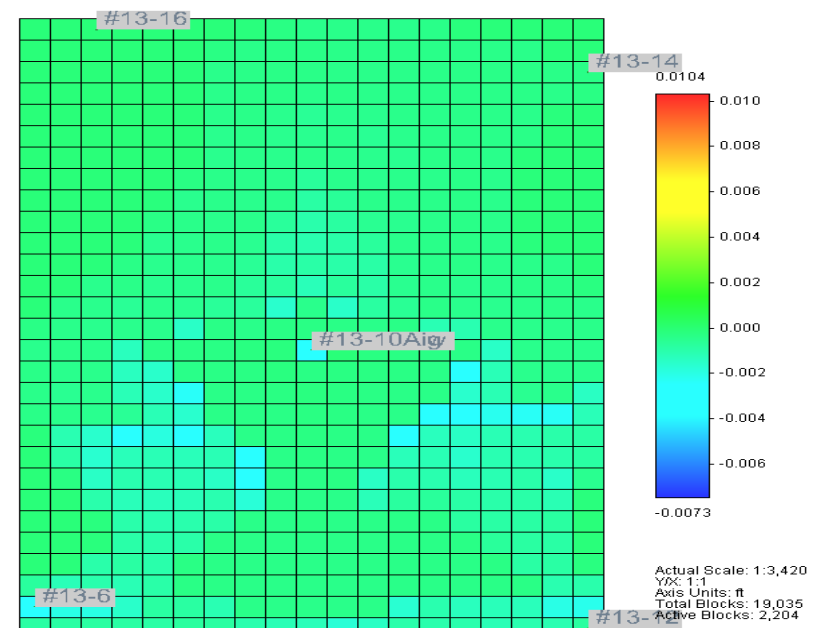
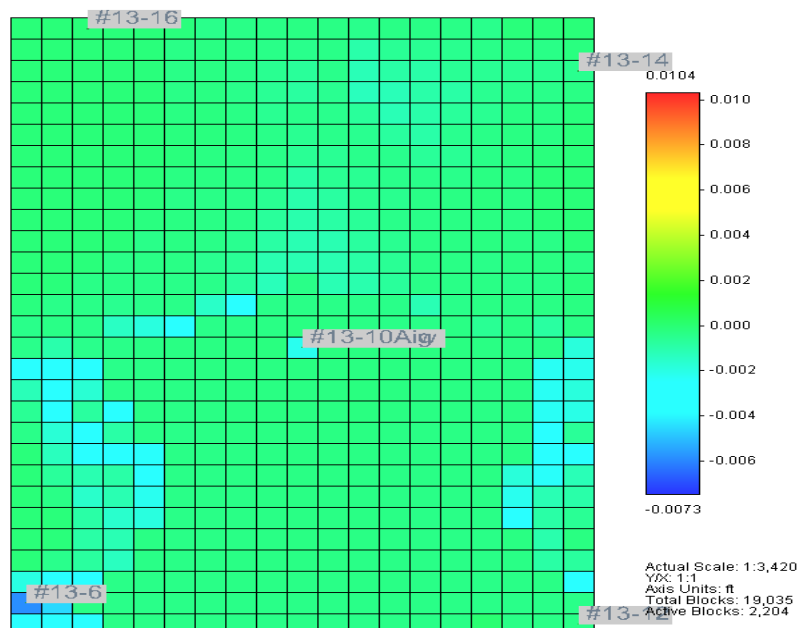
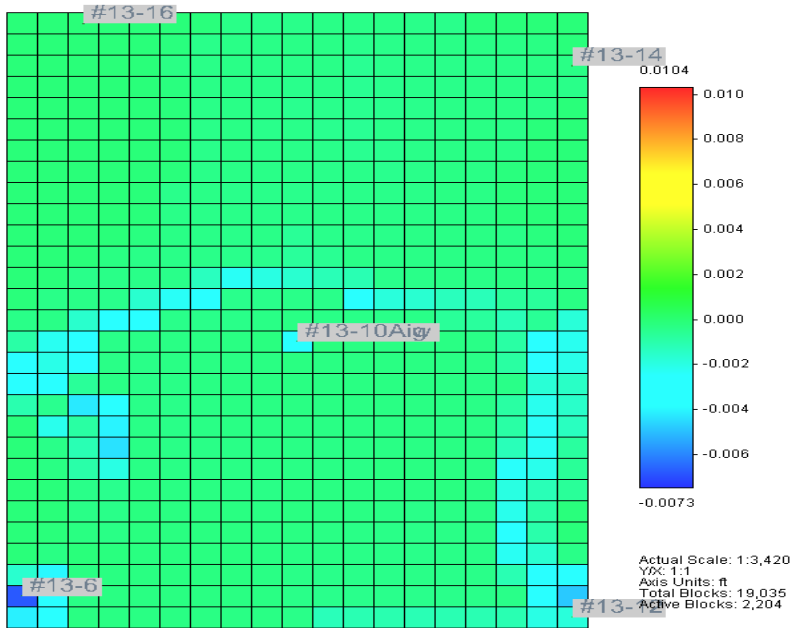


1000 years' impact in layer 10 (3037-Dec-01)

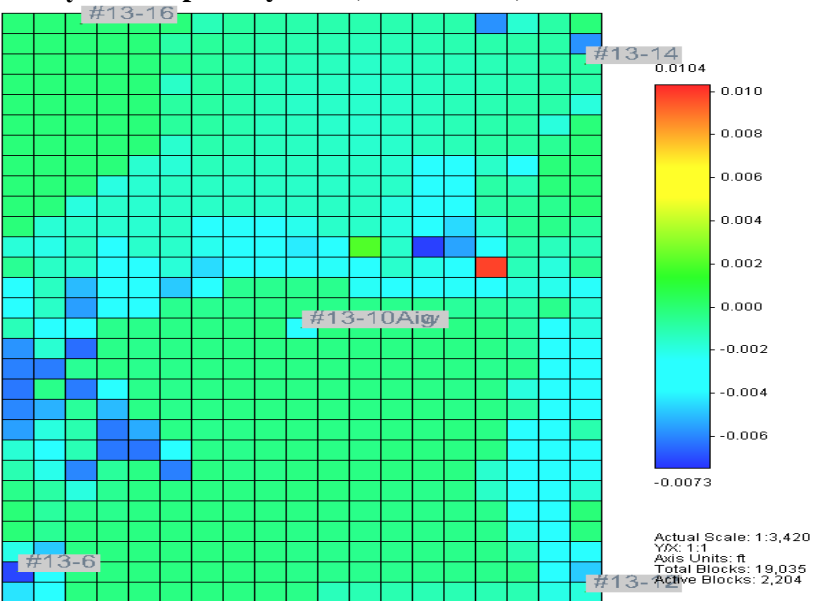
A: Siderite precipitations

B: pH of the reservoir medium

Porosity Variation Heatmaps

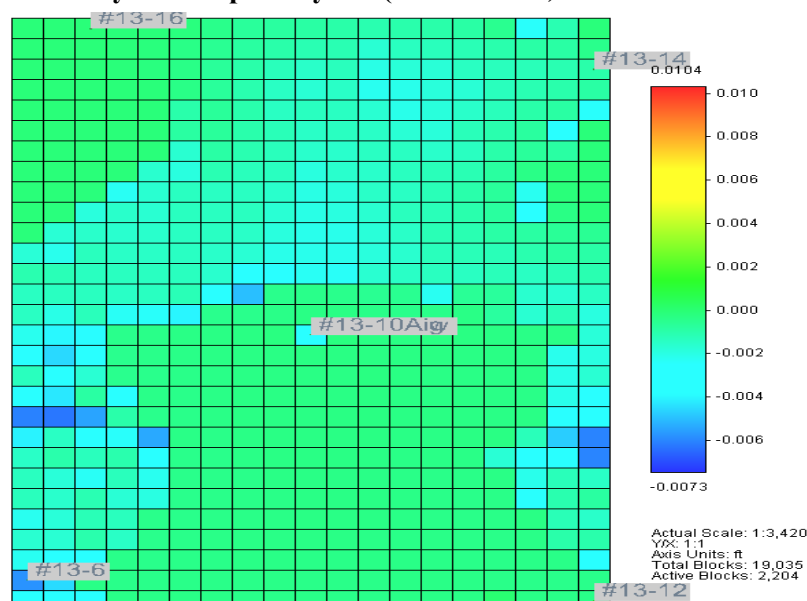


20 years' impact layer 10 (2037-Dec-01)



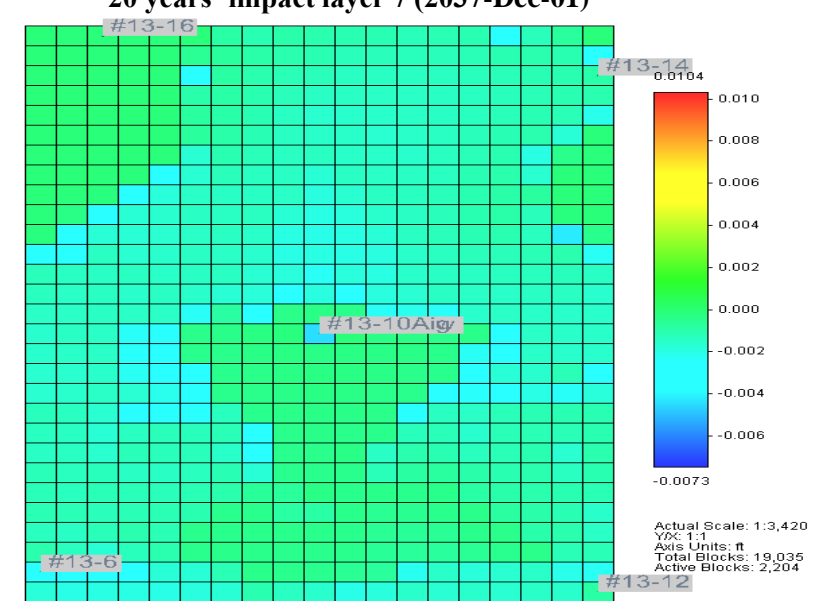
1000 years' impact in layer 10 (3037-Dec-01)

20 years' impact layer 9 (2037-Dec-01)



1000 years' impact in layer 9 (3037-Dec-01)

20 years' impact layer 7 (2037-Dec-01)



1000 years' impact in layer 7 (3037-Dec-01)

Concluding Remarks

1. A fully CO₂-WAG injection strategy guarantees safe storage medium for the injected CO₂ in the Morrow B. Thus, a significant CO₂ was observed to dissolve in the liquid phase as compared with the amount in the structural and residual phase trapping.
2. CO₂ dissolution that accounted for solubility trapping is known to depend on the flow mixture, the amount of the aqueous species, and salinity within the reservoir.
3. The results from the pattern studies also show that the Morrow B is an effective reservoir for CO₂ sequestration and suggest that geochemical storage is highly favorable in both short and long-term.
4. Current work was successfully conducted on the pattern-scale, thus, on a section of the field-scale reservoir. The result suggests ankerite group mineral, Dolomite, shows varying evolution during the study period, while calcite exhibited continuous dissolution. The observed result confirms the flow-through laboratory experiments.
5. The next stage of this work would focus on expanding the simulation work to full field scale.

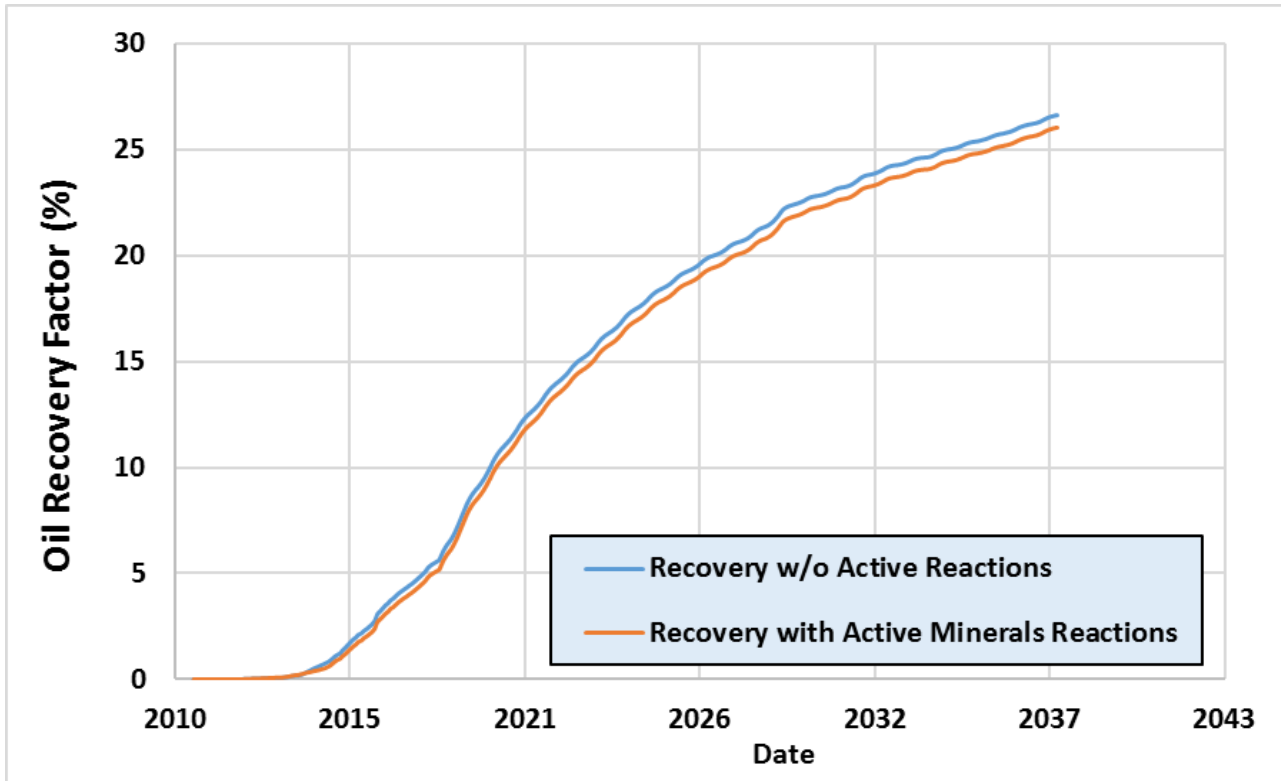
References

1. Ampomah, W., Balch, R. S., Grigg, R. B., Will, R., Dai, Z., & White, M. D. (2016). Farnsworth Field CO₂-EOR Project: Performance Case History. SPE Improved Oil Recovery Conference, 1–18. <https://doi.org/10.2118/179528-MS>
2. Ahmmed, B., Appold, M. S., Fan, T., McPherson, B. J. O. L., Grigg, R. B., & White, M. D. (2016). Chemical Effects of Carbon Dioxide Sequestration in the Upper Morrow Sandstone in the Farnsworth, Texas, hydrocarbon unit. *Environmental Geosciences*, 23(2), 81–93. <https://doi.org/10.1306/eg.09031515006>
3. Riaz Khan, Martin Applod, Brian McPherson, Robert Balch, & Mark White (2017). Evaluation of Geologic CO₂ Sequestration Potential of the Morrow B sandstone in the Farnsworth, Texas Hydrocarbon Field using Reactive transport. [https://netl.doe.gov/sites/default/files/event proceedings/2016/fy16%20cs%20rd/Posters/Appold-Poster.pdf](https://netl.doe.gov/sites/default/files/event%20proceedings/2016/fy16%20cs%20rd/Posters/Appold-Poster.pdf)
4. Palandri, J. L., & Kharaka, Y. K. (2004). A Compilation of Rate Parameters of Water-Mineral Interaction Kinetics for Application to Geochemical Modelling. *U.S. GEOLOGICAL SURVEY Open File Report 2004-1068*, 271(1547), 1–70. <https://doi.org/10.1098/rspb.2004.2754>
5. Pan, F., McPherson, B. J., Esser, R., Xiao, T., Appold, M. S., Jia, W., & Moodie, N. (2016). Forecasting Evolution of Formation Water Chemistry and Long-term Mineral Alteration for GCS in a Typical Clastic Reservoir of the Southwestern United States. *International Journal of Greenhouse Gas Control*, 54, 1–14. <https://doi.org/10.1016/j.ijggc.2016.07.035>
6. Wu, Z. (2018). Chemo-Mechanical Alterations Induced from CO₂ Injection in Carbonate-Cemented Sandstone: An experimental Study at 71 ° C and 290 Bar. Master's Thesis. New Mexico Institute of Mining and Technology

Acknowledgements / Thank You / Questions

Funding for this project is provided by the U.S. Department of Energy's (DOE) National Energy Technology Laboratory (NETL) through the Southwest Regional Partnership on Carbon Sequestration (SWP) under Award No. DE-FC26-05NT42591.

OIL RECOVERY FACTOR AS A FUNCTION OF THE DISPLACEMENT MECHANISMS



- The oil recovery results indicate that the case considering the mineral reactions yields lower oil production.
- Such observation is due to the loss of injected CO₂ via chemical reactions with the insitu brine and formation rocks.

Effect of WAG Cycles on Storage

Prior to Prediction Studies different Injection cycles were tested:

- WAG Cycle with high water injection fraction:
 - Less CO₂ injection
 - Less Recovery
 - Better liquid phase storage
- WAG Cycle of 1:3 yield
 - Highest CO₂ injection
 - Best oil Phase CO₂ storage
 - Lowest Aqueous Phase Storage
- WAG Cycle of 1:2 yield
 - Best recovery, but less injection
 - Highest Storage volumes
 - Best secure storage mediums
 - Met most project objectives

WAG Cycle	Oil Recovery (MM bbl.)	Amount of substances of CO ₂ (10 ⁹ g-moles)					Total Storage
		Total CO ₂ Injection	Structural Trapped gas (Free gas)	Residual Trapped Gas	Solubility		
					Oil	Water	
1:1	10.42	125.89	4.70	4.06	20.90	4.500	34.15
1:2	10.61	155.39	4.78	4.01	21.85	4.457	35.09
1:3	10.47	169.82	4.76	4.04	21.92	4.247	34.96
3:2	10.44	107.31	4.57	3.88	21.63	4.841	34.91
3:1	9.96	80.21	4.17	4.14	18.73	4.840	31.87

Salinity effects on storage

Sea Water

- Massive increase in Na⁺ & Cl⁻
- Lesser CO₂ storage in water

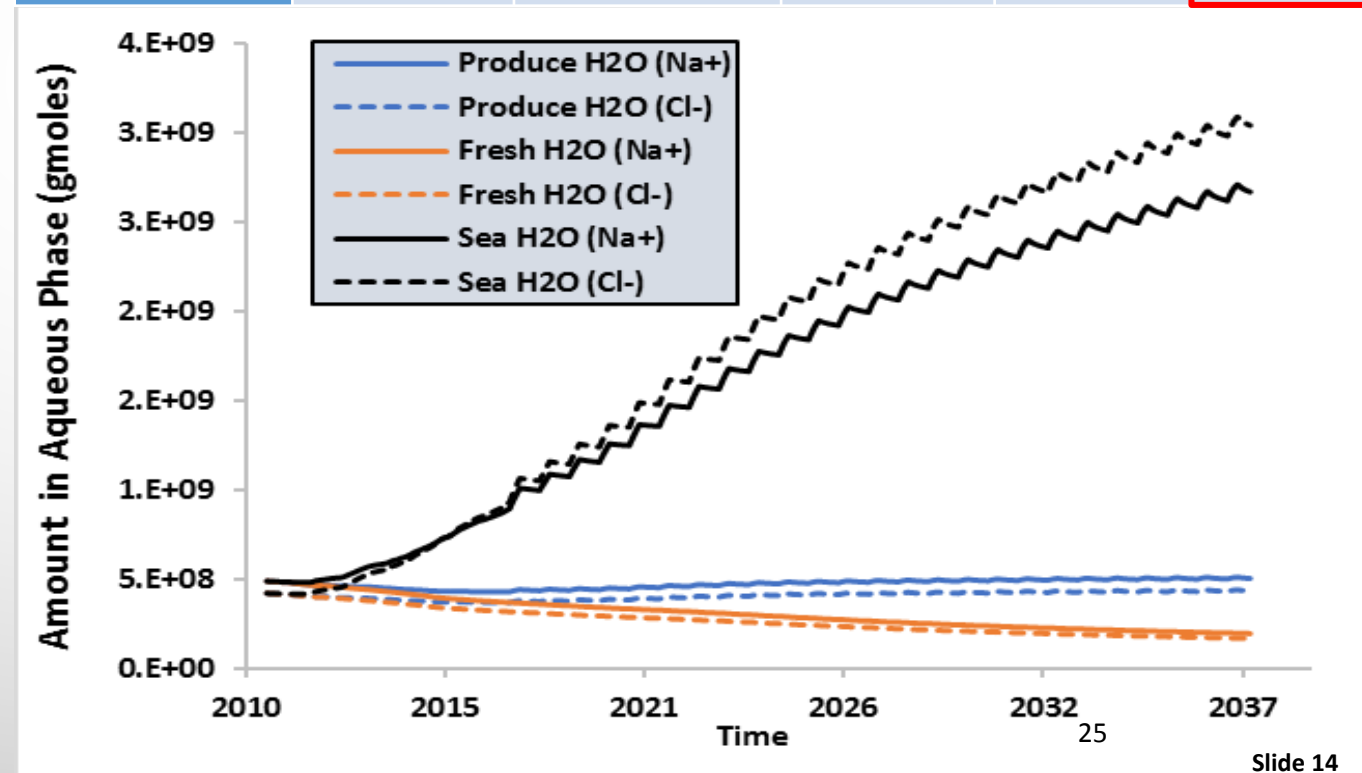
Produced water :

- Slight Increase in Na⁺ & Cl⁻
- Average Storage CO₂ in water
- Highest Oil recovery

Fresh Water:

- Decrease in Na⁺ & Cl⁻
- Highest storage of CO₂ in water
- Less oil recovery
- High water produce
- TDS affect the storage with other species added

Injected Water Type	Oil Recovery (MM bbl.)	Amount of substances of CO ₂ (10 ⁹ g-moles)			
		Structural Trapped Gas (Free gas)	Residual Trapped Gas	Solubility	
				Oil	Water
Seawater	11.815	3.21	2.83	18.75	4.58
Produced Water	12.095	2.83	2.49	18.87	5.05
Fresh Water	11.846	2.72	2.37	18.70	5.09



PERMEABILITY EFFECT FROM GEOCHEMICAL REACTION

$$\hat{\phi}^* = \phi^* - \sum_{\beta=1}^{n_m} \left(\frac{N_{\beta}}{\rho_{\beta}} - \frac{N_{\beta}^0}{\rho_{\beta}} \right)$$

$$\phi = \hat{\phi}^* [1 + c_{\phi} (p - p^*)]$$

$$\frac{K_n}{K_k} = rf = \left(\frac{\phi}{\phi^0} \right)^3 \left(\frac{1 - \phi^0}{1 - \phi} \right)^2$$

ϕ = Porosity

ϕ^* = Reference porosity without mineral precipitation/dissolution

$\hat{\phi}^*$ = Reference porosity including mineral precipitation/dissolution

N_{β} = Total moles of mineral β per bulk volume at the current time

N_{β}^0 = Total moles of mineral β per bulk volume at time 0

ϕ^0 = initial porosity at time 0

n_m = number of minerals

ρ_{β} = mineral molar density

c_{ϕ} = rock compressibility

p^* = reference pressure.

k_n = permeability at current time steps

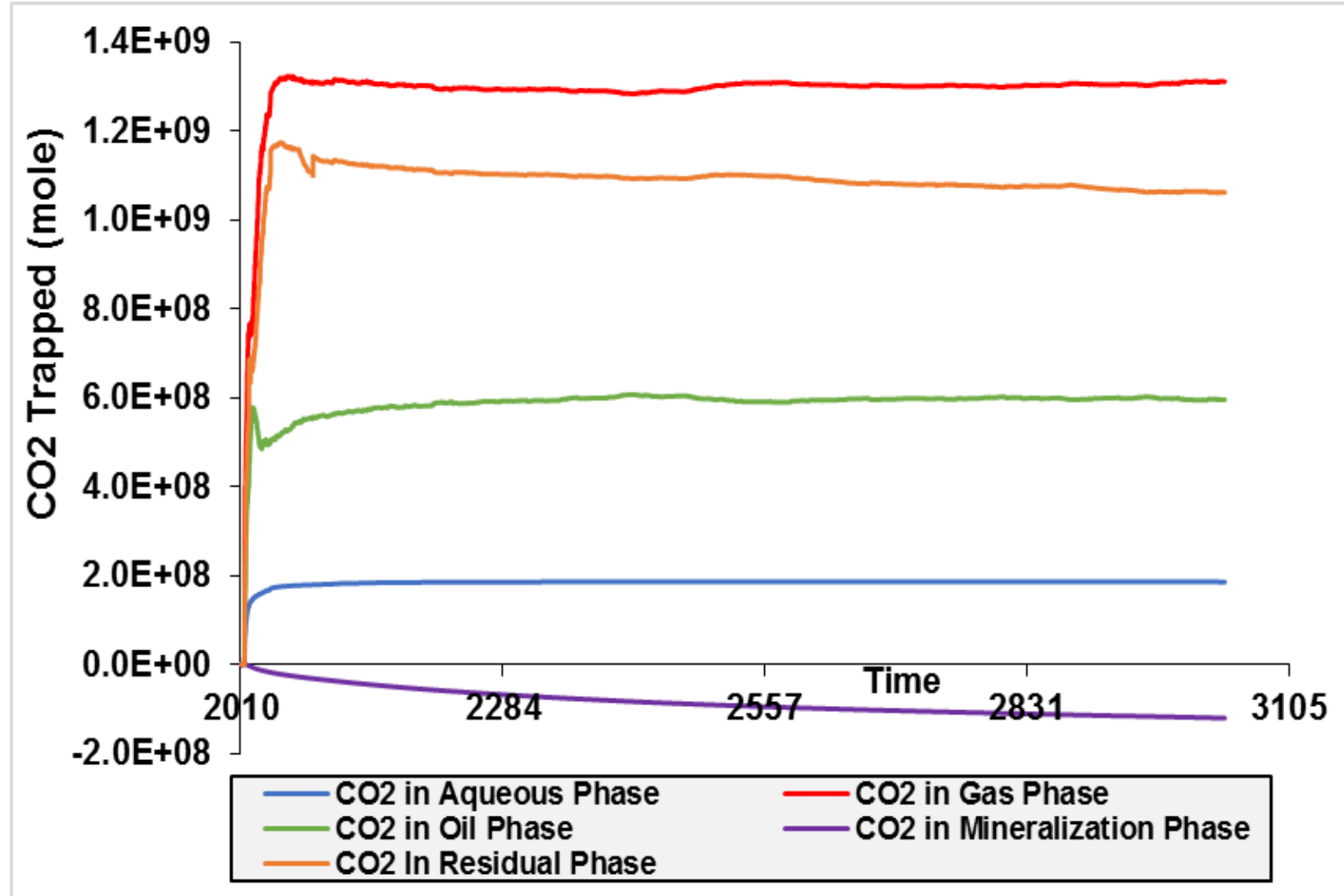
k_k = Initial permeability

rf = Resistance factor

Phase Storage of CO₂ in 13-10A Region

The gradual decrease in residual trapped gas promotes

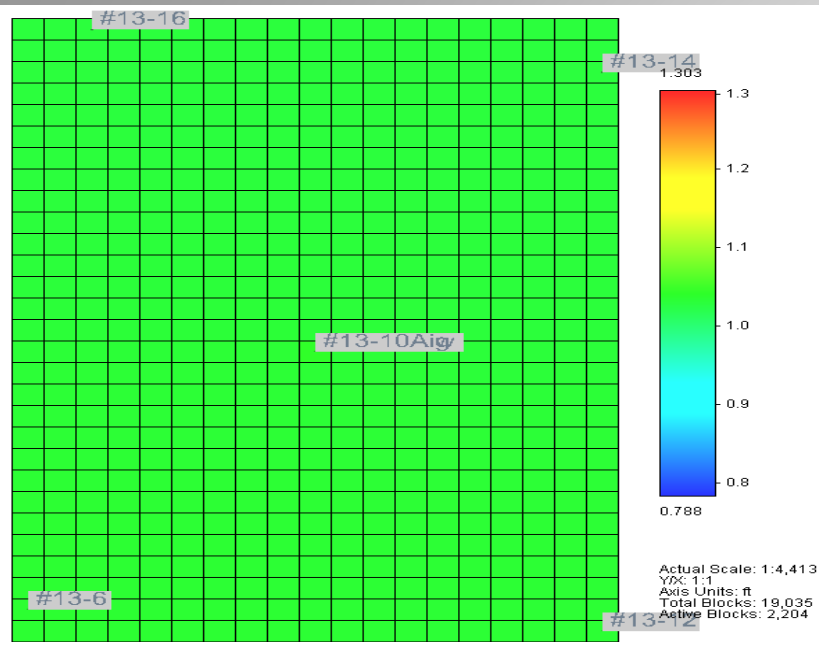
- Mineralization
- Solubility trapping
- In the field-scale, CO₂ dissolution in oil phase is the predominant short-term storage in the FWU



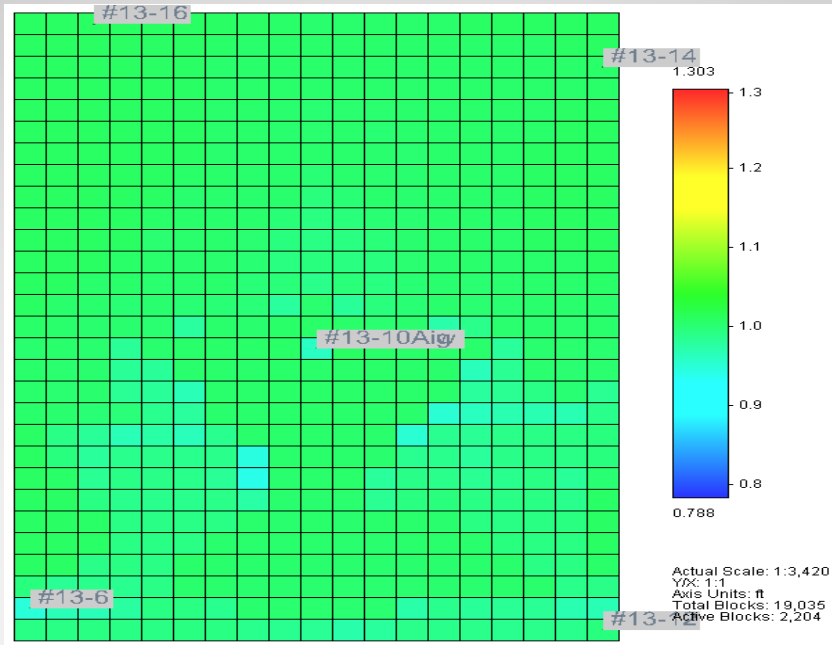
FATE OF INJECTED CO₂ IN MOLES AT 20 YEARS FIELD OPERATION AND 1000 YEARS FIELD MONITORING PERIOD

Components	During 20 years Operation	1000 years (After Shut-In)
1. CO _{2(aq)}	1.1019E+08	1.6505E+08
2. CO ₃ ²⁻	3.20E+04	6.20E+04
3. HCO ₃ ⁻	1.1016E+08	1.64987E+08
4. Albite	-1.40E+07	-8.76E+07
5. Quartz	3.98E+07	1.78E+08
6. Calcite	-1.71E+06	-6.45E+06
7. Dolomite	9.66E+05	-2.05E+07
8. Siderite	3.43E+07	5.94E+07
9. Illite	9.51E+04	-7.08E+06
10. Kaolinite	1.30E+07	7.58E+07
11. Smectite	-2.02E+06	-2.89E+06

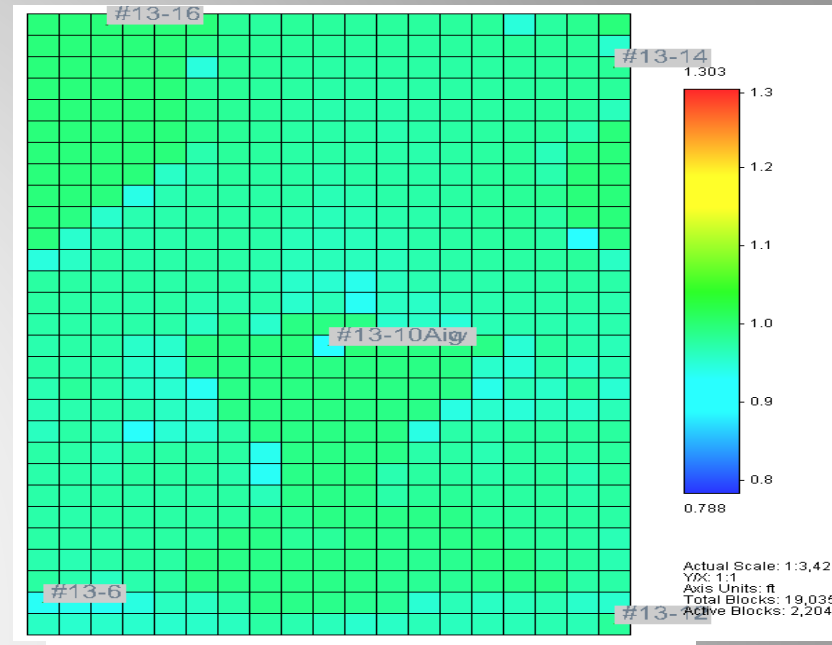
OIL PERMEABILITY RESISTANCE FACTOR



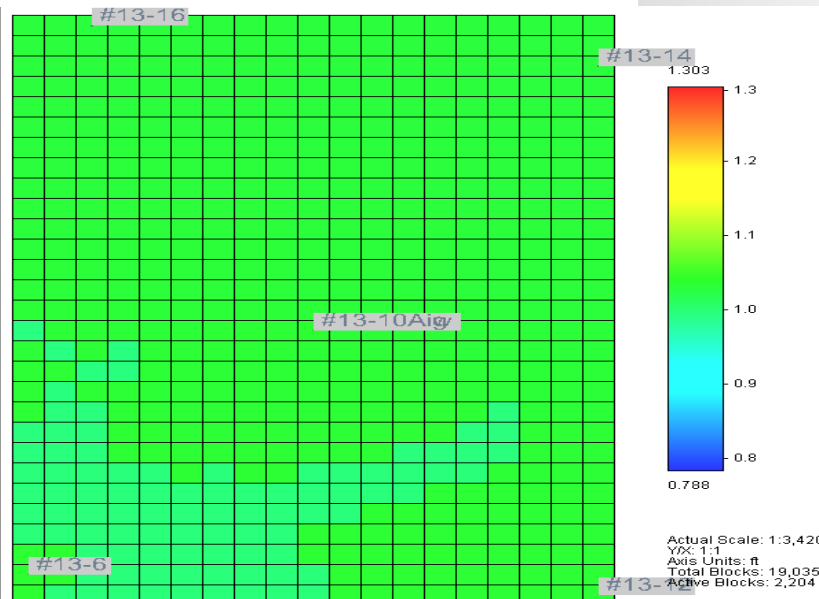
4 years Impact in most layer 7,8,9 (2014-Jan-01)



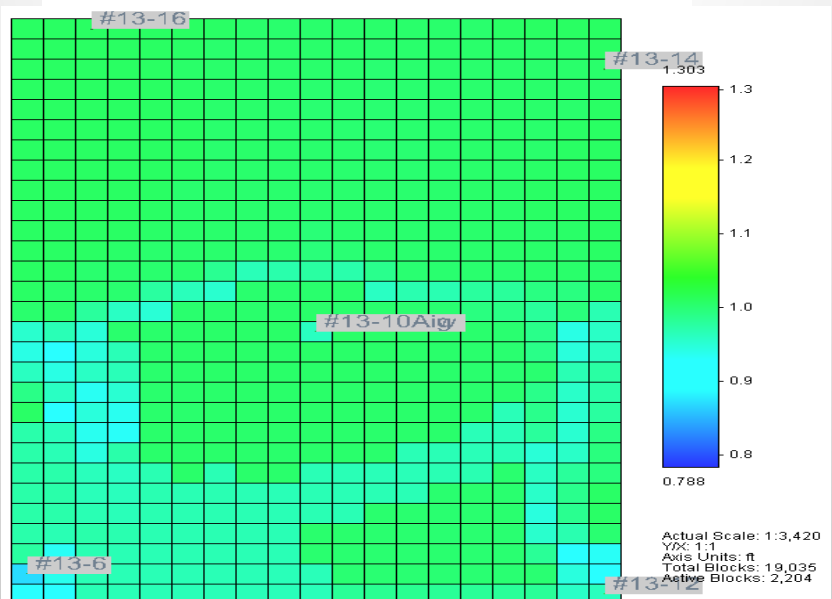
20 years' impact in layer 7 (2037-Dec-01)



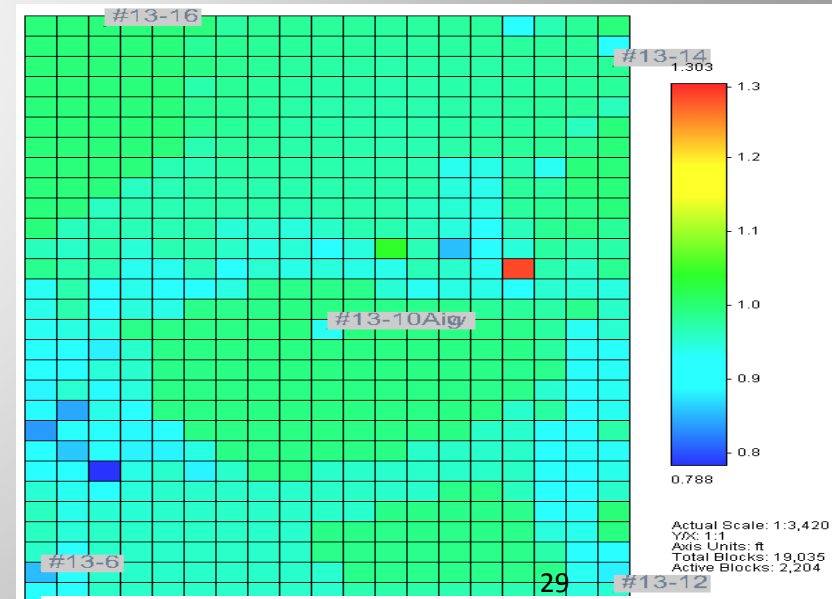
1000 years' impact in layer 7 (3037-Dec-01)



4 years' impact in layer 10 (2014-Jan-01)



20 years' impact in layer 10 (2037-Dec-01)



1000 years' impact in layer 10 (3037-Dec-01)